

Article

From Waste to Potential Reuse: Mixtures of Polypropylene/Recycled Copolymer Polypropylene from Industrial Containers: Seeking Sustainable Materials

Carlos Bruno Barreto Luna ^{1,*}, Wallisson Alves da Silva ², Edcleide Maria Araújo ¹,
Lara Júlia Medeiros Dantas da Silva ¹, João Baptista da Costa Agra de Melo ² and Renate Maria Ramos Wellen ³

¹ Academic Unit of Materials Engineering, Federal University of Campina Grande, Av. Aprígio Veloso, 882-Bodocongó, Campina Grande 58429-900, Brazil; edcleide.araujo@ufcg.edu.br (E.M.A.); lara_julia2010@hotmail.com (L.J.M.D.d.S.)

² Academic Unit of Mechanical Engineering, Federal University of Campina Grande, Av. Aprígio Veloso, 882-Bodocongó, Campina Grande 58429-900, Brazil; wallissonalves11@hotmail.com (W.A.d.S.); joao.agra@ufcg.edu.br (J.B.d.C.A.d.M.)

³ Department of Materials Engineering, Federal University of Paraíba, Cidade Universitária, João Pessoa 58051-900, Brazil; wellen.renate@gmail.com

* Correspondence: brunobarretodemauufcg@hotmail.com

Abstract: This work investigated the effect of thermo-oxidation aging in blends of copolymer polypropylene (PPc)/recycled copolymer polypropylene (PPcr) from industrial container waste, coded as PPc/PPcr blends. All compounds were melt extruded, and the injection molded specimens were characterized by mechanical properties (tensile and impact), Fourier-transform infrared spectroscopy (FTIR), melt flow index (MFI), contact angle, heat deflection temperature (HDT), differential scanning calorimetry (DSC), and scanning electron microscopy (SEM). FTIR spectra presented bands related to the hydroperoxides and carbonyl groups, as resulted from thermo-oxidation aging. The contact angle decreased upon a thermo-oxidation aging influence, corroborating the FTIR spectra. PPcr presented higher MFI as a consequence of reprocessing. Impact strength and elongation at break were quite sensible to the thermo-oxidation aging influence and were progressively reduced upon increased time, whereas tensile strength, elastic modulus, and HDT only slightly changed. SEM images of PPc presented a higher quantity of pulled-out particles, resulted from a lower interaction between phases, i.e., polypropylene and ethylene/propylene. From the impact strength and toughness data, proper dissipation energy mechanisms were found in PPc/PPcr blends. Summing up, using PPcr contributed to minimize properties' losses, which may be related to the stabilizer agents, whereas the described results presented great potential for the PP market, while contributing to the sustainable environment.

Keywords: polypropylene; industrial containers; waste; mechanical recycling; polymer blends



Citation: Luna, C.B.B.; da Silva, W.A.; Araújo, E.M.; da Silva, L.J.M.D.; de Melo, J.B.d.C.A.; Wellen, R.M.R. From Waste to Potential Reuse: Mixtures of Polypropylene/Recycled Copolymer Polypropylene from Industrial Containers: Seeking Sustainable Materials. *Sustainability* **2022**, *14*, 6509. <https://doi.org/10.3390/su14116509>

Academic Editors: Dong Tian, Shuangqiao Yang and Qingye Li

Received: 1 March 2022

Accepted: 11 April 2022

Published: 26 May 2022

Publisher's Note: MDPI stays neutral with regard to jurisdictional claims in published maps and institutional affiliations.



Copyright: © 2022 by the authors. Licensee MDPI, Basel, Switzerland. This article is an open access article distributed under the terms and conditions of the Creative Commons Attribution (CC BY) license (<https://creativecommons.org/licenses/by/4.0/>).

1. Introduction

Polypropylene (PP) is one of the most important thermoplastics in the polymer industry, with a wide range of applications; it is a relatively lower cost resin, with low density, good processability, corrosion resistance, high crystallinity, and excellent permeability to water and CO₂, properties that are translated into one of the most worldwide-consumed polymers [1–4]. Nevertheless, the large production, together with inappropriate discharge, have contributed to seriously damage the environment, mainly in big cities, where flooding and urban pollution are clearly seen [5–7]. As a proper solution, mechanical recycling has been encouraged, which, additionally, allows for the pre-reevaluation of PP waste [8].

Mechanical recycling is a common practice in the polymer industry to reprocess plastics, usually using extruders or injectors [9]. Recycled materials can be mixed with virgin

resin to obtain better properties at reduced cost [10]. At the same time, using plastic waste as a raw material for new products reduces the waste accumulation, heading to a cleaner environment [11,12], which, together with the lack of landfills and economic aspects, are proper justifications to encourage efforts to promote the plastic recycling [13–15]. Therefore, research is focused on polymer recycling, based on blends and composites from reused commodity polymers [16–18], which currently have wide applications in the industry, especially, due to the proper balance between stiffness and toughness [19].

Ferreira et al. [20] developed mixtures based on polypropylene homo polymer (PP) with recycled PP (PPr) (Big Bag fabric waste), compounded in a co-rotating twin screw extruder. Thermal, mechanical, and thermo-mechanical properties as well as morphology were investigated, in order to evaluate the optimum concentration. It was observed that upon addition of 10% and 50% of PPr, properties settled down, whereas compounds with 30% PPr presented the best properties' balance at a lower cost, evidencing that the residue can be properly reused.

Mechanical properties, as the tensile and impact strength of blends based on PP/ethylene-propylene/PPr, were investigated by Fernandes and Domingues [21]; it was verified at 30% PPr that a satisfactory mechanical properties' balance for bumper application was reached, whereas at higher PPr content decreased mechanical properties were collected, being translated into lower quality products.

Barbosa et al. [22] investigated the effect of secondary recycling on PP samples, so tensile and impact tests were performed. From the gathered data, the tensile properties of PP and PPr were similar, as well as the developed blends. However, the impact strength of the PPr and PP/PPr blends was lower than that of PP, indicating PPr can replace PP in tensile-requested applications but not in impact ones.

PP/PPr blends have received significant technological interest due to their good mechanical properties and cost effectiveness. Consequently, mechanical, thermal, and rheological properties as well as morphology have been constantly investigated by the academic and industrial communities. However, a few found research articles are based on the effect of thermo-oxidation aging in PPc/PPcr blends, which is relevant, since post-consumption PP may have stabilizing additives that are added to minimize the losses of the mechanical properties and degradation during processing [23]. In this case, adding PPcr into the production of PPc/PPcr blends can lead to savings in additives on the final product and, at the same time, keep mechanical properties at high levels.

When reusing and manufacturing PPcr products, nature preservation is provided and pollution reduced, in addition with the energy savings, since it replaces part of the virgin resin [24]. Hence, the process also contributes to the recycling industry's growth and leads to new employment opportunities. Therefore, PPcr reuse appears, as a smart alternative to this raw material, to reincorporate into the production and reduce the environmental impact. Consequently, this practice directly contributes to sustainable development.

Based on the above mentioned, this work aimed to evaluate the thermo-oxidation aging effect on PPc/PPcr blends with 20%, 40%, and 60% PPcr, mechanical (tensile, impact), thermal (DSC), and thermo-mechanical properties (HDT), so chemical modifications (FTIR), surface change (contact angle) and microstructure (SEM) were carefully investigated.

2. Materials and Methods

2.1. Materials

Copolymer polypropylene (PPc), coded as EP440P, with density of 0.895 g/cm³ and MFI of 17 g/10 min (230 °C/2.16 kg), were supplied as pellets and manufactured by Braskem. This copolymer has a PP matrix and ethylene/propylene as a dispersed phase. Post-consumer polypropylene (PPcr, where "r" refers to recycled), with density 0.904 g/cm³ (ASTM D792), was obtained from industrial containers from local companies in Campina Grande-PB (Brazil). These industrial containers are manufactured with PPc, i.e., a PP matrix with a dispersed phase of ethylene/propylene.

2.2. Methods

PPcr cleaning and milling PPcr containers were submitted into the separation process to remove the adhesive labels, afterwards, they were ground with a knife mill to reach flakes shape, which were washed in water to remove contaminants and dried in a vacuum oven at 60 °C for 24 h. Figure 1 shows a schematic representation to acquire the recycled material.

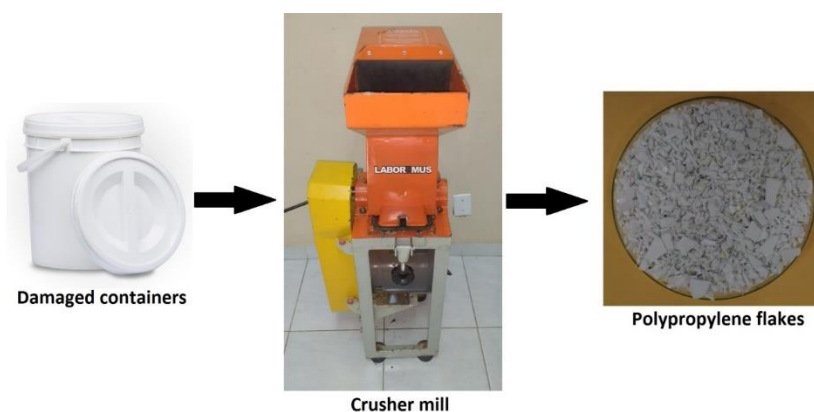


Figure 1. Schematic representation of the applied method to obtain the recycled material [10].

2.3. Blend Processing

PPc and PPcr were dry blended at PPc/PPcr (80%/20%); PPc/PPcr (60%/40%); and PPc/PPcr (40%/60%) contents. Afterwards, the blends were processed into a Coperion Werner-Pfleiderer model ZSK (D = 18 mm and L/D = 40) modular co-rotating twin-screw extruder, at 190 °C in all zones, with a screw rate of 250 rpm and feed rate of 3 kg/h, and a thread profile configured with distributive and dispersive mixing elements. Neat PPc and neat PPcr were processed using the same conditions as the blends, for comparative purposes. The extruder output was pelletized and dried in a vacuum oven for 24 h at 60 °C. Specimens were injection molded using an Arburg Model Allrounder 207C Golden Edition injector, applying the informed parameters in Table 1. Before testing, specimens were sealed and stored in a desiccator for 48 h. Impact strength as well as tensile and heat deflection temperature (HDT) specimens were determined, following ASTM D256 (Type I), D638, and D648, respectively.

Table 1. Injection parameters.

Parameters	
Injection pressure (bar)	1000
Temperature profile (°C)	170; 170; 170; 180; 180; 180; 190
Mold temperature (°C)	20
Cooling time inside the mold (s)	30
Holding pressure (bar)	500

Figure 2 shows a schematic flowchart of the processing performed in the laboratory.

2.4. Thermo-Oxidation Aging

Thermo-oxidative aging was conducted in a circulating air oven at 70 °C, for 30 and 60 days; afterwards, specimens were tested.

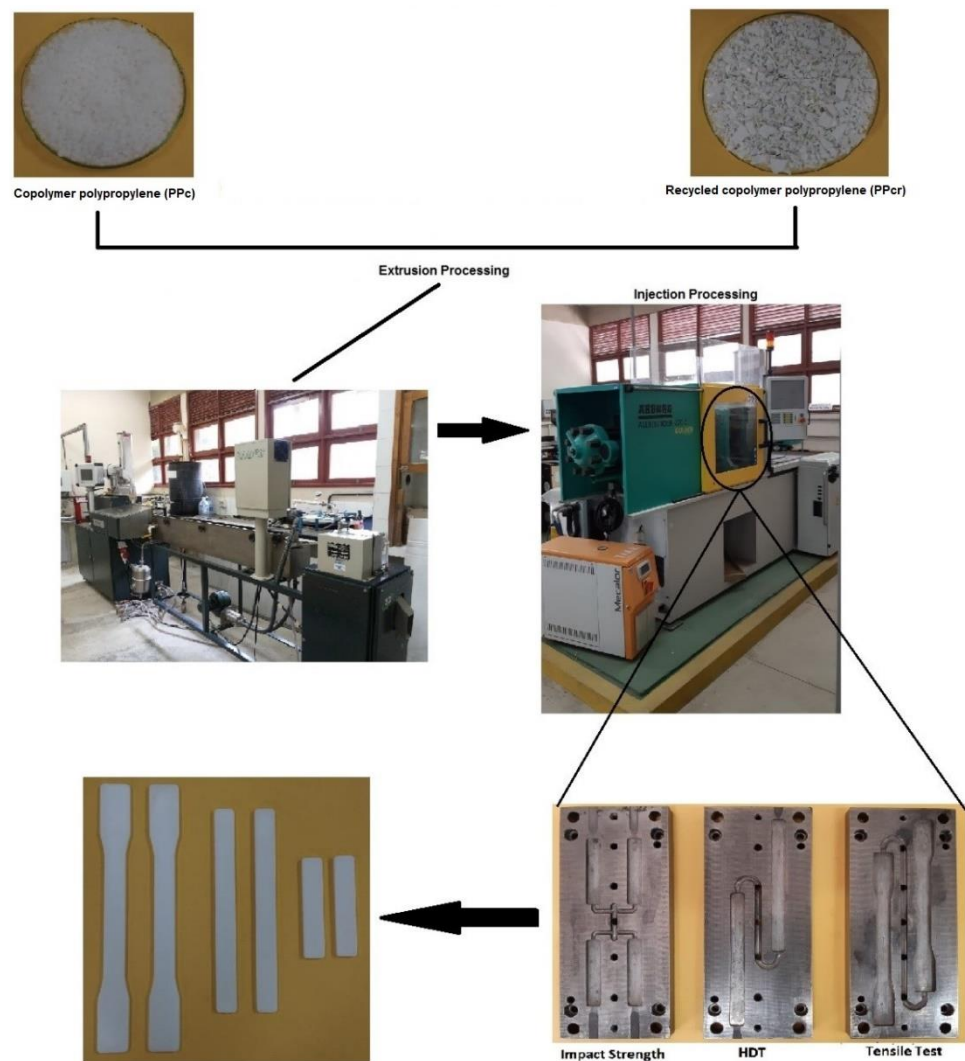


Figure 2. Schematic representation of extrusion processing and injection molding [10].

2.5. Characterization

Fourier-transform infrared spectroscopy (FTIR) was performed using a Perkin Elmer FTI/ATR Spectrum 400 Spectrometer (attenuated total reflectance), with scan range from 4000 to 650 cm^{-1} , 32 scans at 4 cm^{-1} resolution.

Contact angle analysis was performed by the sessile drop method, using a portable contact angle, the Phoenix-i model from Surface Electro Optics (SEO). The distilled water drop was deposited on an impact test specimen using a micrometric dozer, and the captured images were analyzed by the software associated with the equipment. Images were captured, using intervals of 200 s, from thermo-oxidation-aged surface specimens at 0, 30, and 60 days.

The Izod impact strength test was performed on notched specimens, according to ASTM D256, in a Resil 5.5 J from Ceast, operating with a hammer of 2.75 J, at room temperature (~ 23 °C). Presented results are the average of five specimens.

The tensile test was carried out with injected specimens according to ASTM D638, using an EMIC DL 2000 universal test machine with elongation rate of 50 mm/min and load cell of 5 kN at room temperature (~ 23 °C). Presented results are the average of five specimens.

Melt flow index (MFI) tests were performed using a plastometer, model DSM MI-3, according to the ASTM D-1238 standard, with a load of 2.16 kg at 230 °C. The samples

were collected after 10 s of flow, and the reported results were analyzed with the average of ten samples.

Heat deflection temperature (HDT) was performed according to ASTM D648, in a Ceast HDT 6 VICAT model with voltage of 455 kPa and heating rate of 120 °C/h. The temperature was determined after the specimen was deflecting 0.25 mm. Presented results are the average of three specimens.

Differential Scanning Calorimetry (DSC) analysis was performed in a DSC-Q20 from TA Instruments. The scans were evaluated from 30 to 200 °C, under a heating rate of 10 °C/min and a gas flow rate of 50 mL/min, in a nitrogen atmosphere; samples with approximately 5 mg were tested.

Scanning electron microscopy (SEM) analyses were performed on the fractured surface of impact specimens. A Shimadzu SSX-550 Superscan was used at a voltage of 15 kV under high vacuum. The investigated fractured surfaces were gold coated.

3. Results and Discussion

3.1. Processing Aspects

Figure 3 shows the extruded granules and the as-injected specimens of PPc, PPcr, and blends. During extrusion, it was found that PPcr and PPc/PPcr blends, regardless of the recycled material content, did not affect the processability related to PPc. The extruded material (PPc, PPcr, and blends), called “spaghetti”, was practically constant and continuous, and melting fracture was not observed. This behavior indicates viscosity stability during processing. Apparently, although PPcr is a recycled material, there was no thermomechanical degradation, since the color remained white, as shown in Figure 3. PPc showed a lighter hue, while the blends followed the PPcr trend, having a whiter hue. The higher degree of opacity for PPcr and PPc/PPcr blends is mostly due to the added additives to the recycled material, as well as the higher degree of crystallinity, as verified by the DSC data. In this case, scattering of visible light occurred at the boundaries between the crystalline and amorphous regions, and the higher crystallinity increased the intensity of the light scattering, which leads to greater opacity [25].

During injection, PPc, PPcr and blends presented similar behavior; the mold was completely filled and specimens without defects were collected. Apparently, PPc/PPcr blends needed less time to fill the mold, related to PPc. This behavior indicates the higher melt flow index (MFI) of PPcr provided a reduced filling time into the mold.

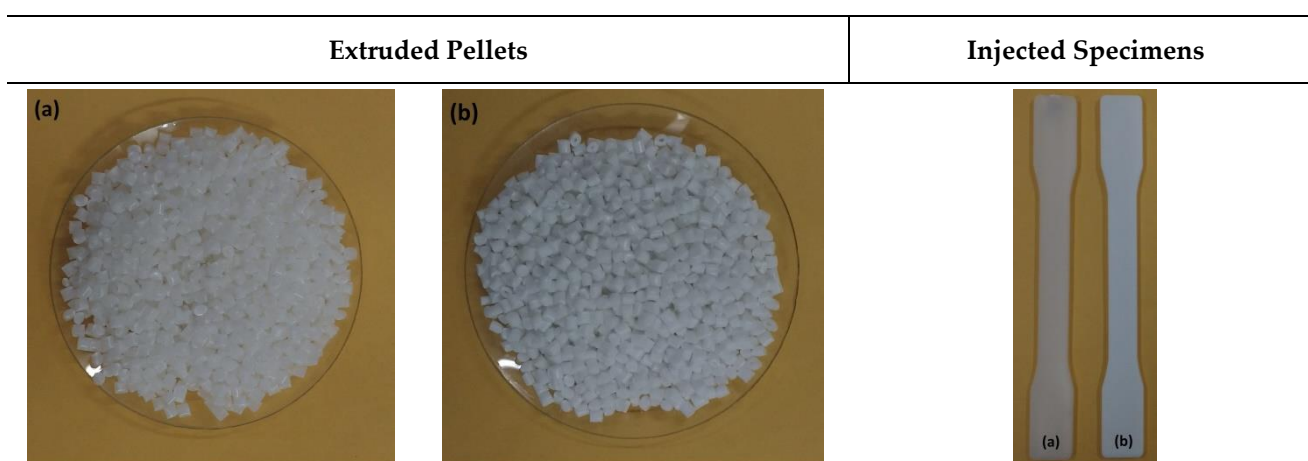


Figure 3. Cont.

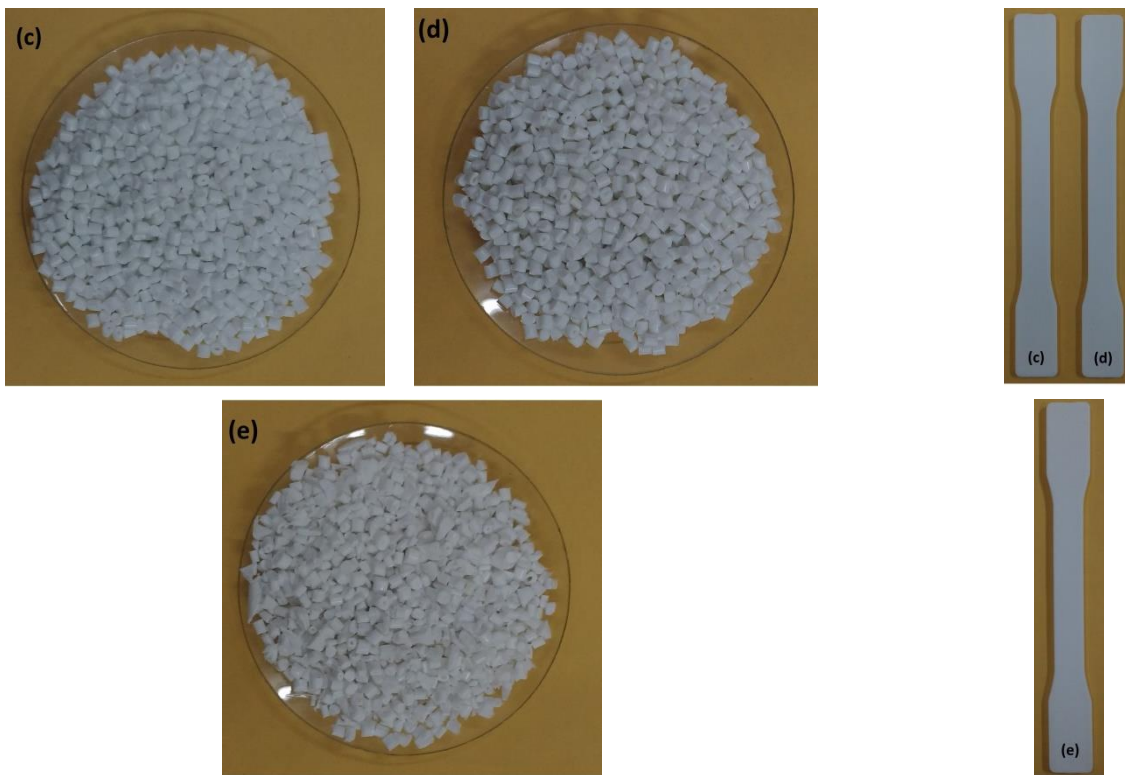


Figure 3. Pellets from extrusion and injected specimens: (a) PPc; (b) PPc/PPcr (20%); (c) PPc/PPcr (40%); (d) PPc/PPcr (60%); and (e) PPcr.

3.2. Fourier-Transform Infrared Spectroscopy (FTIR)

FTIR Spectroscopy is a powerful technique to analyze the chemical changes on PP structure that have arisen from the thermo-oxidation aging influence, thus allowing assessment of the degradation intensity [26].

Figure 4 shows the FTIR spectra of PPc, PPcr, and PPc/PPcr blends, non-aged and aged for 30 and 60 days, respectively. In the spectra of non-aged PPc and PPcr, the main PP bands were observed at 808 cm^{-1} , due to the angular deformation of the out-of-plane C-H; at 841 cm^{-1} and 1168 cm^{-1} , corresponding to C-C isopropyl stretching; and at 974 and 1000 cm^{-1} , due to C-C stretching of CH_2 and CH_3 groups [27,28], respectively. The band at 1304 cm^{-1} corresponds to CH_2 vibrations; at 1375 and 1455 cm^{-1} , due to the symmetrical and asymmetrical angular deformations, respectively, of CH_3 [29,30]. The bands in the region $2839\text{--}2917\text{ cm}^{-1}$ correspond to the aliphatic $-\text{CH}$ stretching (CH_2 and CH_3) [31] and, at 2721 cm^{-1} , the characteristic band of PP ($-\text{CH}_3$) [32].

At 0 days of thermo-oxidation aging, no significant changes related to the degradation of PPc, PPcr and PPc/PPcr blends were verified in the presented spectra; they are quite similar, showing absence of carbonyl and hydroperoxide groups, without severe degradation evidence during processing (PPc, PPc/PPcr) and reprocessing (PPcr) [33]. It is believed PPcr may have stabilizer agents, as commonly used in PP industrial processing, to reduce the degradation rate and increase the product life [34]. Therefore, it is reasonable to suggest the presence of such additives would have minimized the generation of new oxidative groups during reprocessing, i.e., extrusion and injection.

Under the thermo-oxidation aging effect, the FTIR spectra in Figure 4 present broad bands in the region between $3000\text{--}3700\text{ cm}^{-1}$, since the intensity increases for longer times, they are associated with hydroperoxides [35], i.e., unstable groups easily decomposed, which may start PP degradation. As a by-product of these reactions, carbonyl groups ($\text{C}=\text{O}$) are formed, which are the main chemical group from PP degradation [36], usually leading to mechanical properties' losses, as presented further on in Figures 10–15.

The carbonyl groups (C=O) are observed in the range between 1800 and 1600 cm^{-1} [37], since the intensity increases with thermo-oxidation aging, indicating PP degradation is taking place. PPc is composed of ethylene-propylene as a dispersed phase (Figure 4a), which favors crosslinking reactions associated with the ethylene group [38,39]. Therefore, chain scission and crosslinking reactions take place during the thermo-oxidation aging of PPc, PPcr, and PPc/PPcr blends; although the chain scission is the predominant mechanism in PP (matrix), crosslinking reactions may take place due to the ethylene groups [40,41]. Tochacek et al. [42] showed that the predominant degradation in polypropylene is chain scission, however, the ethylene/propylene rubber phase suffered the crosslinking mechanism.

At 60 days of thermo-oxidation aging, new bands arose from the degradation processes, with a pronounced increase in the band of the carbonyl group. Apparently, PPc presented the highest intensity for the carbonyl band; meanwhile, although lower in PPcr spectra, its carbonyl band is observed as a double peak in the range between 1800 and 1600 cm^{-1} , suggesting the origin of new chemical subgroups [43]. PPc/PPcr blends showed intermediary changes linked to the neat polymers, specifically for the blend with 60% PPcr, with the carbonyl double peak observed in the same range, i.e., between 1800 and 1600 cm^{-1} , indicating it is PPcr-content dependent.

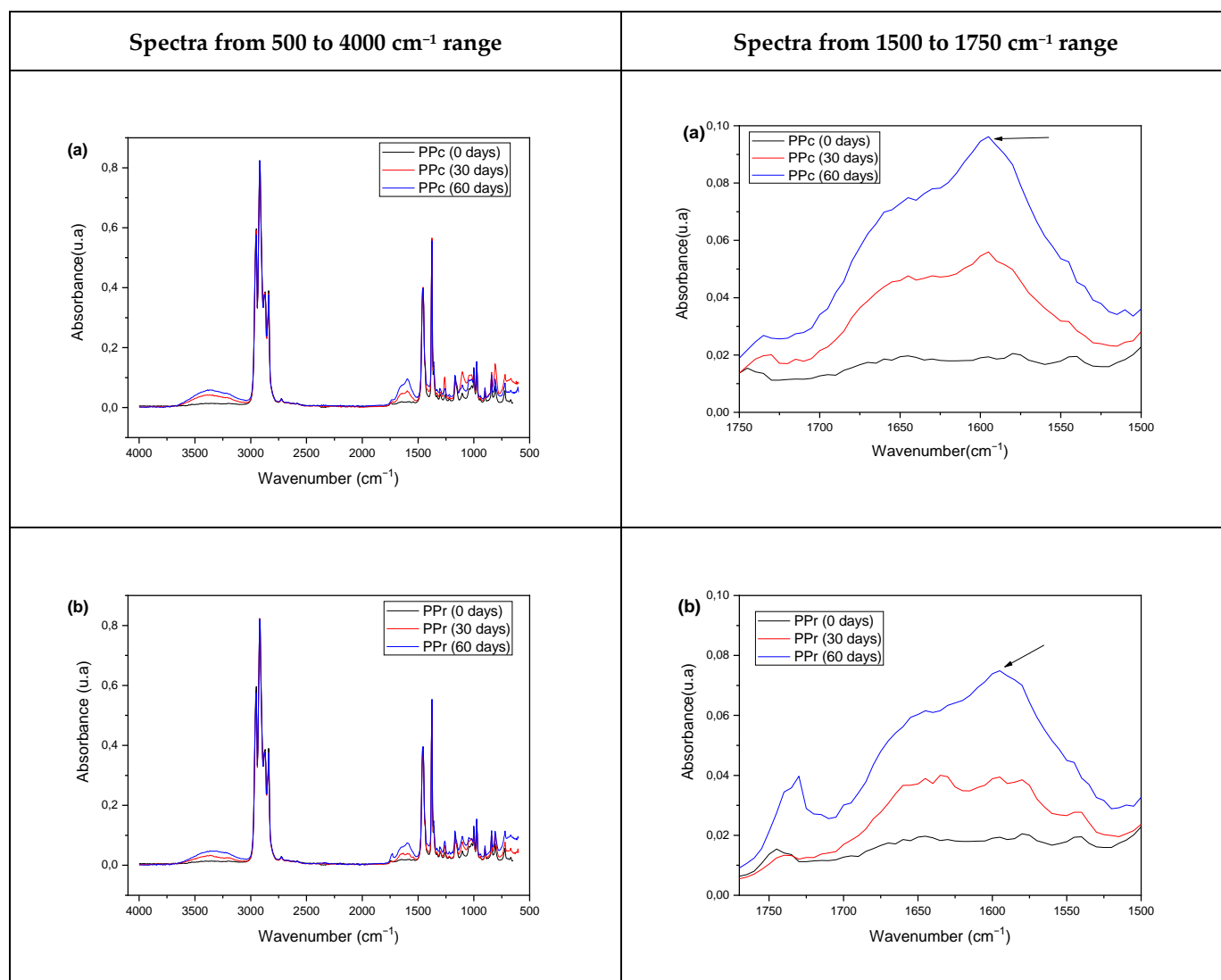


Figure 4. Cont.

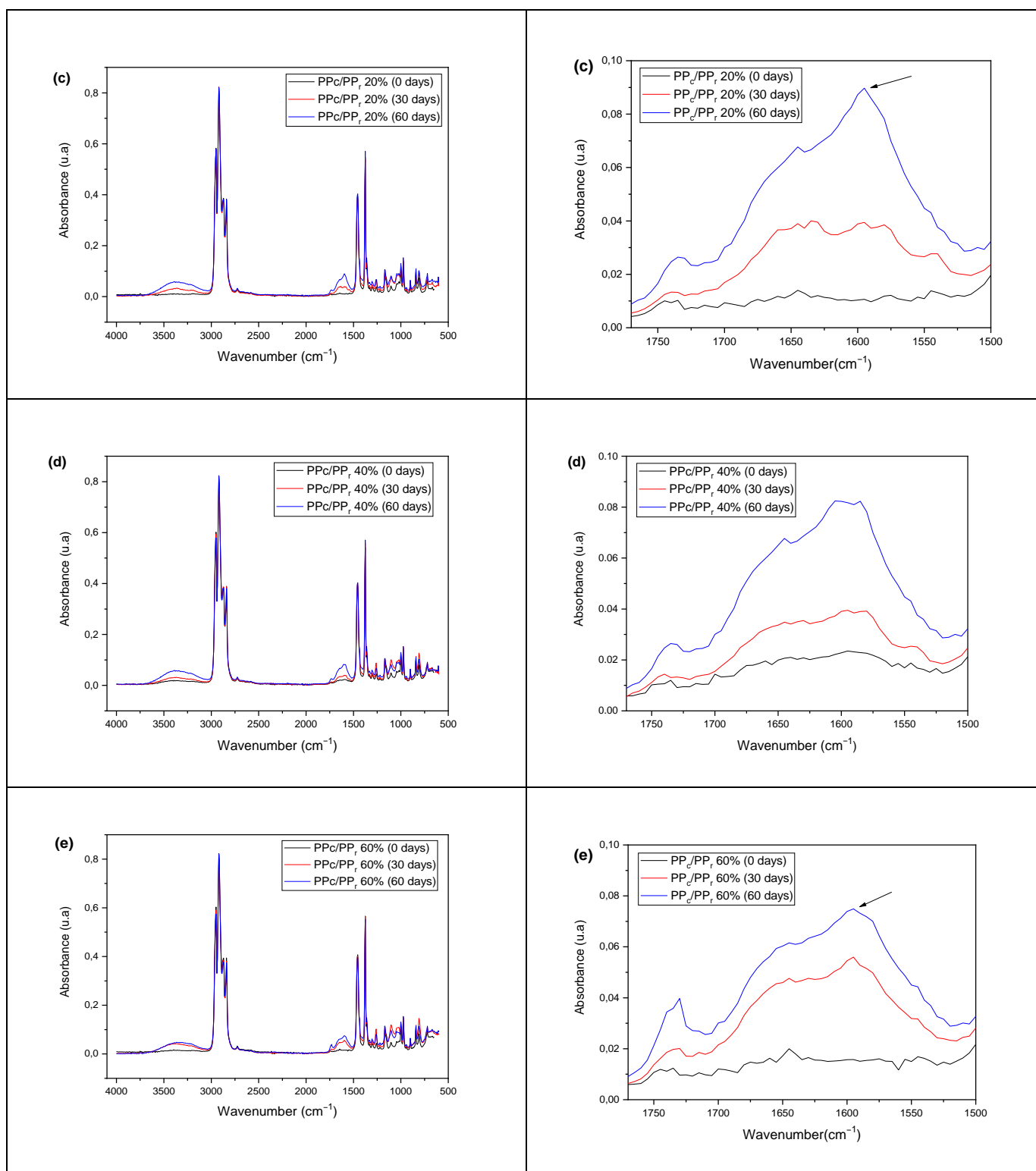


Figure 4. FTIR spectra of specimens before and after thermo-oxidation aging: (a) PPc; (b) PPcr; (c) PPc/PPcr (20%); (d) PPc/PPcr (40%); (e) PPc/PPcr (60%). Thermo-oxidation aging times indicated.

The literature [37,44] indicates the region between 1850–1550 cm^{-1} is typical of carbonyl groups, as seen in Figure 4 (zoom in, on the right side). Quantification of carbonyl absorption was performed by the absorbance measurement of the total area relative to the highest peak (arrow indicated), as proposed in the literature [45]. The underlying area of the most intense peak was also accounted for in the calculation of the carbonyl

index. Figure 5 shows the evolution of carbonyl absorbance as function of thermo-oxidation aging time. At 30 days of aging, PPc and PPc/PPcr blends presented lower absorbance of carbonyl groups related to PPc, with the exception of the blend with 60% PPcr. For longer aging periods (60 days), PPc showed the highest absorbance of the carbonyl group, suggesting that the degradation is more severe in the virgin material. During 60 days of aging, there was an inverted behavior with PPc/PPcr blends (60%), since the absorption band was close to PPcr, which indicates that for longer aging periods, the greater amount of PPcr in the blends contributed to delay the degradative effects, confirming the lower losses in impact strength and elastic modulus, as presented further on.

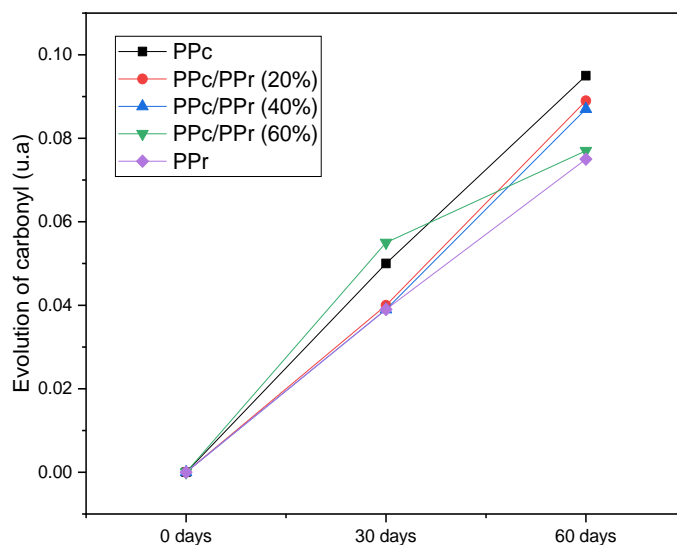


Figure 5. Average variation on the absorbance of the carbonyl band as a function of thermo-oxidation aging.

PPcr is industrial reprocessed, and, even so, did not present carbonyl groups before aging, according to Figure 4b (0 days). This finding suggests that the stabilizer (antioxidant) presence is able to prevent or reduce aging effects and degradation during processing, as already reported [30,34]. Indeed, if PPcr had undergone severe degradation during reprocessing, discoloration and dark tonality are expected on injected specimens [46] which did not happen, as presented in Figure 3e. An important consequence of a PPcr addition to PPc/PPcr blends is the fact that it minimizes the degradative effects during extrusion and injection, as well as during thermo-oxidation aging, as presented in Figure 5. As direct consequence, the mechanical properties will suffer less deleterious effects. Therefore, reusing PPcr has become interesting for PPc/PPcr blends' development, since it reduces the virgin resin via the recycled one. At the same time, there is the advantage of utilizing ecological materials to contribute to sustainable development.

3.3. Contact Angle

Contact angle has been an added parameter to evaluate wettability changes on polymers' surface, due to the degradation mechanisms. The greater the contact angle between the water drop and the surface is, the higher the polymer hydrophobicity [47,48]. Figure 6 presents contact angle images of PPc, PPcr, and PPc/PPcr blends, before and after the thermo-oxidation aging intervals. Initially, PPc presented the largest contact angle (95.5°), and PPcr presented the lowest one (60.7°), while the blends presented intermediate values, as expected by the additive rule. Upon the thermo-oxidation aging influence, the contact angle reduced and surfaces became more hydrophilic. It is suggested chemical reactions took place, producing hydroperoxides and carbonyl groups, which provide higher polarity surfaces [49]; therefore, the hydrophilic character increased, corroborating spectra modifications as verified through FTIR.

Upon thermo-oxidation aging progress from 30 to 60 days, the contact angle decreased, suggesting the increase in degradation. Nevertheless, for the PPc contact angle the reduction was more severe, decreasing 31.6% after 60 days, whereas PPcr diminished to 13.7%. PPc/PPcr blends presented a contact angle at intermediary values related to neat polymers, indicating PPcr presents higher thermo-oxidation degradation stability, which delays the formation of carbonyl and hydroxyl groups. It is believed PPcr may have antioxidant, which reacts as a thermal oxidation retardant [50].

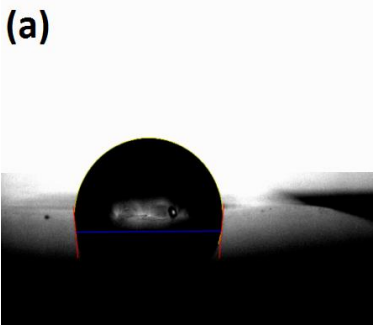
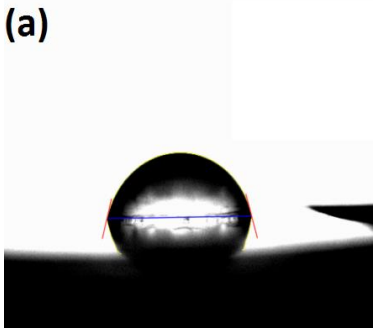
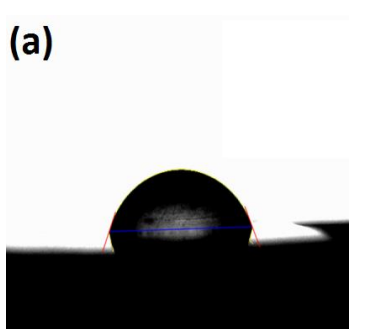
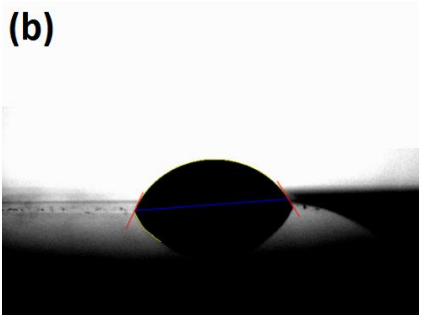
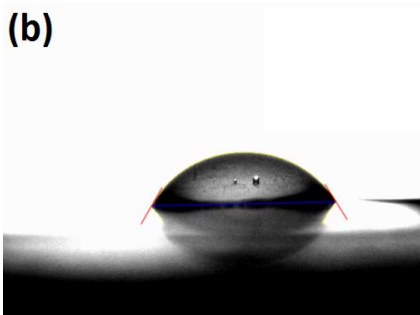
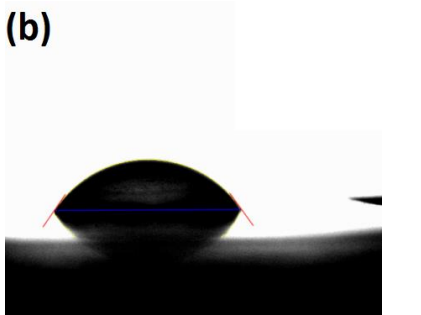
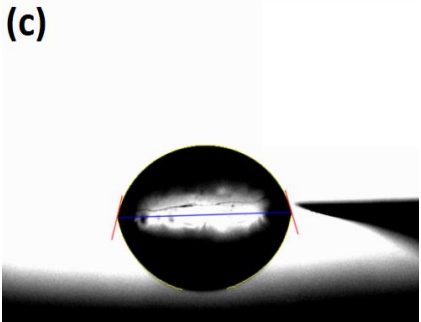
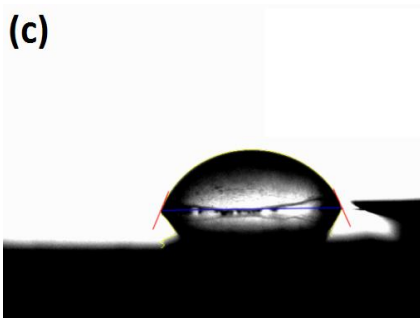
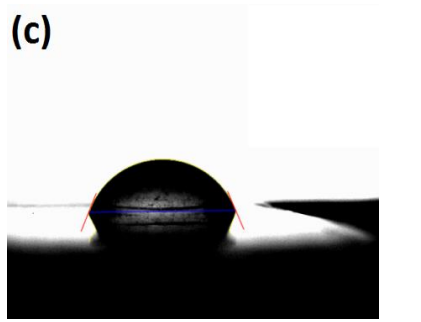
0 days	30 days	60 days
95.5 ± 2.0	74.1 ± 0.4	65.3 ± 0.3
(a) 	(a) 	(a) 
60.7 ± 0.5	58.8 ± 0.7	52.4 ± 0.4
(b) 	(b) 	(b) 
74.1 ± 0.6	67.6 ± 0.6	65.8 ± 0.8
(c) 	(c) 	(c) 
61.9 ± 0.4	61.3 ± 0.5	58.2 ± 0.5

Figure 6. Cont.

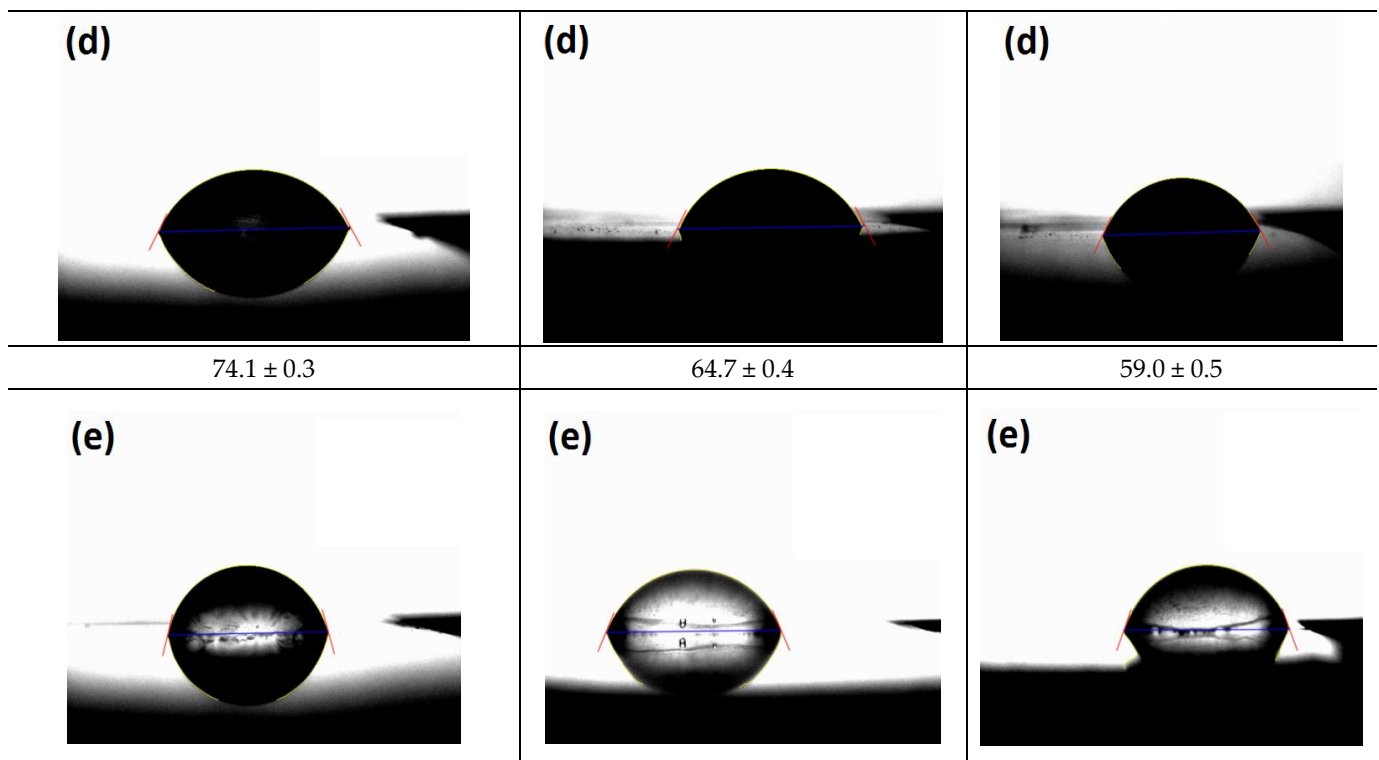


Figure 6. Contact angle images captured from the dripped water droplets on the specimen surface and captured after 200 s for: (a) PPc; (b) PPcr; (c) PPc/PPcr (20%); (d) PPc/PPcr (40%); (e) PPc/PPcr (60%).

3.4. Scanning Electron Microscopy

The phase behavior and properties of polymeric systems are closely related [51], so based on this fundament, the effect of thermo-oxidation aging on the morphology of PP samples was analyzed through SEM images, as shown in Figure 7. PPc, PPcr, and non-aged blends presented typical morphologies of immiscible systems with phase separation, and biphasic morphology is observed, with spherical particles of ethylene/propylene as the dispersed phase in the PP matrix. Ductile fracture (plastic deformation) is observed which corroborates high impact strength as presented in Figure 10.

Aiming to increase toughness, dispersed elastomeric phase is generally used in the PP matrix [52]. Presented morphology of neat PPc and neat PPcr, Figure 7a,b, indicates that, in the PP matrix, a balanced amount of ethylene/propylene dispersed configures an essential point for toughness. In fact, the literature [34,53] indicates when PPc has a very high content of propylene, a miscible blend is formed with the PP matrix. In this case, there is no formation of dispersed particles, and, consequently, the toughness mechanism is not effective. On the other hand, in more balanced proportions of ethylene/propylene (44–48%/52–56%), the dispersed phase is formed reaching a high impact strength for PP, as seen in Figure 10. Apparently, the morphology of not-aged PPc (0 days) showed a larger quantity of dispersed particles of ethylene/propylene in the PP matrix, as related to PPcr. As a result, there is a greater energy dissipation capacity under the impact of PPc than related to PPcr.

In Figure 7b, it should be noted PPcr has the typical morphology of a toughened material [54], which is similar to that of PPc, since it was used to manufacture industrial containers. In general, there is homogeneity in the particle size of the dispersed phase, in addition to voids, due to some particles of the dispersed phase that were removed from the PP matrix.

In the SEM images of PPc, PPcr, and blends, voids are observed from the pulled-out particles of ethylene/propylene during the impact test, which resulted from lower interaction between phases, indicative of low-miscibility compounds. Morphological changes

took place during thermo-oxidation aging: for PPc, there was a significant reduction in the attached ethylene/propylene particles, suggesting a higher stiffness on the elastomeric phase, resulting in decreased energy absorption, i.e., lower impact strength. In this case, it is possible that another process may have occurred during aging, concurrent with PP chain scission, probably crosslinking associated with ethylene/propylene, similar to the HDPE degradation process [55].

From SEM images of PPc, white particles are verified (circled in black) for 30 and 60 days, which may be associated with: (1) impurities in PPc, as it is a recycled material; (2) by-products derived from degradation; or (3) additives' migration during aging.

The blends, regardless of the recycled material content, presented similar morphologies to the non-aged ones. White particles (circled in black) are observed, suggesting being derived from PPc, nevertheless, these particles do not seem to have severe deleterious effect on the mechanical properties, since no significant losses were displayed.

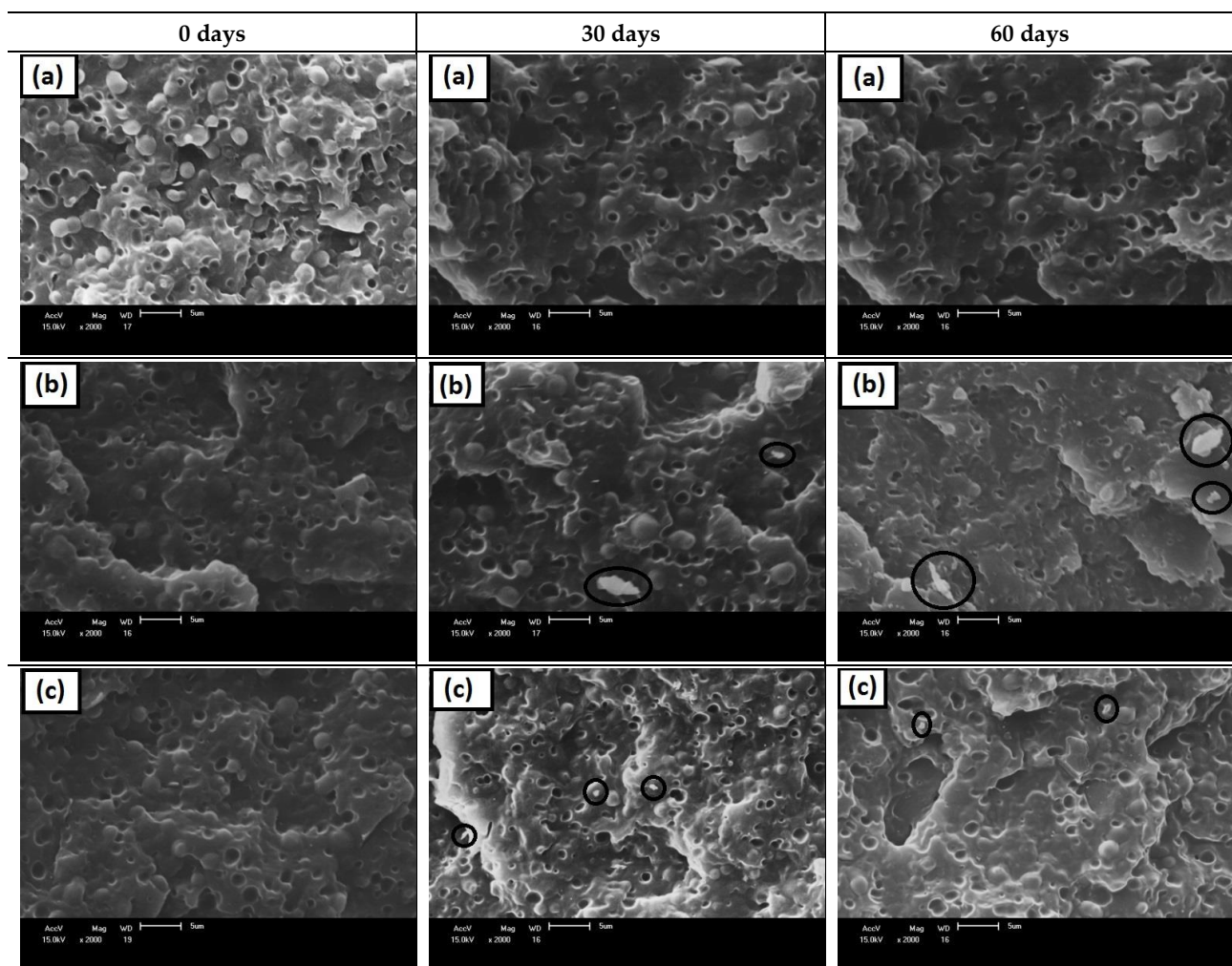


Figure 7. Cont.

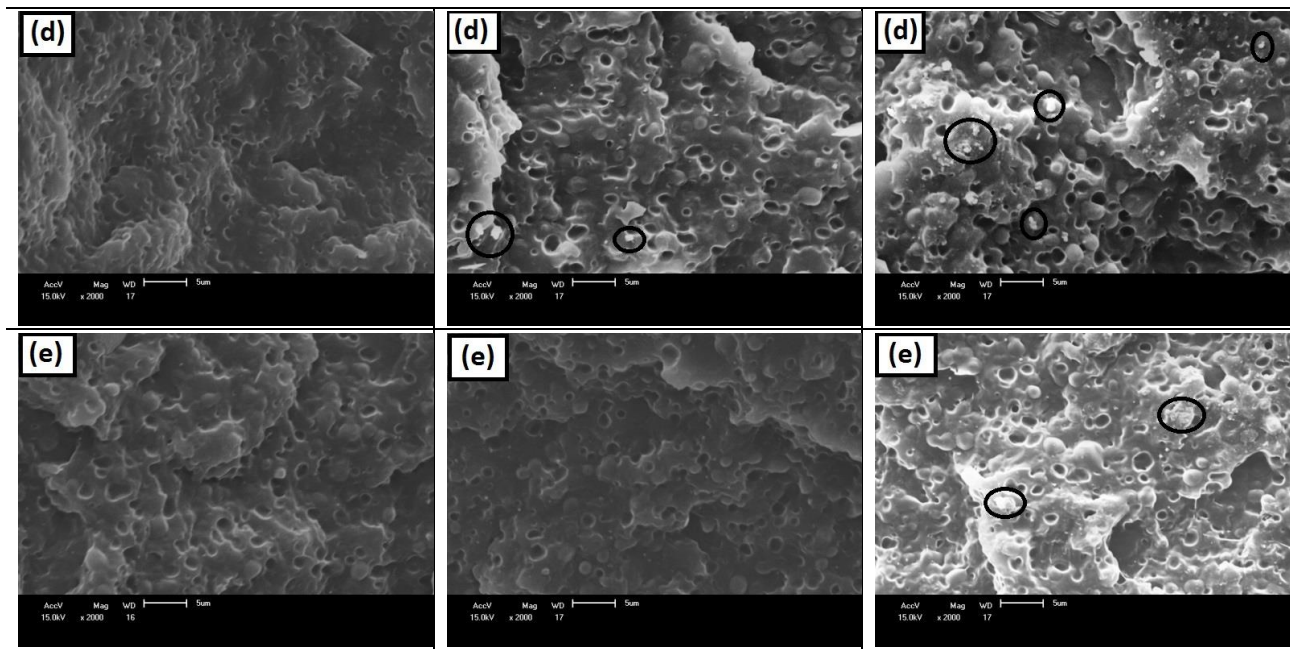


Figure 7. SEM images for: (a) PPc; (b) PPcr; (c) PPc/PPcr (20%); (d) PPc/PPcr (40%); (e) PPc/PPcr (60%).

3.5. Melt Flow Index (MFI)

Figure 8 presents MFI data for PPc, PPcr, and PPc/PPcr blends, and in general the non-aged samples presented a lower MFI, indicating higher viscosity and higher molecular weight; among them, PPc presented the lowest one (17.9 g/10 min), i.e., the most viscous with the highest molecular weight, whereas PPcr presented the highest MFI (35 g/10 min), suggesting a lower molecular weight. In fact, generally, during reprocessing cycles, chain scission takes place, resulting in reduced macromolecular chains [56], an assumption clearly verified for PPcr, which provided blends with a higher MFI. The thermo-oxidation aging causes an MFI increase; samples became more fluid, suggesting a lower molecular weight. The literature [57,58] has presented, under degradation, that the chain scission is the predominant mechanism on PP's macromolecules. Nevertheless, as in the present work, PPc (copolymer) is used, so it is reasonable to assume both mechanisms may take place, i.e., chain scission and reticulation (crosslinking reactions), even at a slight degree [59], which could provide counterbalanced mechanisms, avoiding deeper damages in PPcr and Pc/PPcr blends, as shown in Figure 8. As there was no drastic change in the MFI due to the thermo-oxidation aging on PPc, PPcr, and PPc/PPcr blends, it is reasonable to suggest that a complex mechanism is occurring in the degradation, i.e., the PP matrix is undergoing chain scission, while the dispersed ethylene/propylene phase is probably undergoing low-intensity crosslinking, as already proposed [60,61].

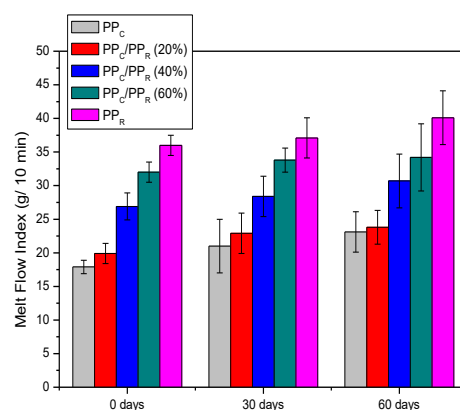


Figure 8. MFI for PPc, PPcr, and PPc/PPcr blends.

3.6. Differential Scanning Calorimetry

The DSC parameters of PPc, PPcr, and blends, computed during the second heating and cooling, are presented in Table 2, whereas the DSC scans acquired during the second heating and cooling are in Figure 9.

Table 2. PPc, PPcr, and PPc/PPcr blends melting and crystallization parameters before and after thermo-oxidation aging.

PPc	0 Days	30 Days	60 Days	PPcr	0 Days	30 Days	60 Days
T_m (°C)	165.0	169.4	170.2	T_m (°C)	167.7	168.0	167.9
ΔH_m (J/g)	71.4	55.1	45.6	ΔH_f (J/g)	75.2	74.6	73.8
T_c (°C)	122.9	121.2	120.1	T_c (°C)	121.6	122.0	121.9
X_c (%)	34.5	26.6	22.0	X_c (%)	36.3	36.0	36.1
PP/PPcr (20%)	0 days	30 days	60 days	PP/PPcr (40%)	0 days	30 days	60 days
T_m (°C)	166.0	168.0	169.0	T_m (°C)	165.5	169.6	167.9
ΔH_m (J/g)	75.9	59.0	48.9	ΔH_f (J/g)	78.1	58.9	51.6
T_c (°C)	123.0	122.8	122.3	T_c (°C)	122.8	120.2	121.1
X_c (%)	36.7	28.5	23.6	X_c (%)	37.7	28.4	24.9
PP/PPcr (60%)	0 days	30 days	60 days				
T_m (°C)	165.3	169.8	168.7				
ΔH_m (J/g)	75.5	54.7	62.1				
T_c (°C)	122.9	120.2	121.3				
X_c (%)	36.5	26.4	30.0				

T_m = Melting peak temperature; T_c = crystallization temperature; ΔH_m = Melting enthalpy; X_c = Degree of crystallinity, $X_c = \Delta H_m / \Delta H_m^0$, where: ΔH_m^0 = Enthalpy of 100% crystalline PP, in this work 207 J/g [62].

Before thermo-oxidation aging, PPc presented T_m 165 °C, as is usual for PP and attributed to the melting of the crystalline α phase (Ferreira et al., 2019), while PPcr and PPc/PPcr blends presented slightly higher T_m ; as PPcr is a lower-viscosity polymer (please see MFI data in Figure 8), it is believed crystallization and ordering phenomena were improved due to easier macromolecular chain mobility being translated in higher perfection crystals and T_m [63,64].

PPcr and non-aged blends show a slight increase in the melting enthalpy related to PPc; mostly due to higher crystallinity. This finding is important for polymer recycling, since when just using a recycled material in high concentrations, gains in mechanical and thermomechanical properties are reached, as presented further on. However, reversal behavior in the melting enthalpy is observed upon aging for 30 and 60 days. As aging progresses, PPc and blends presented reduced melting enthalpy. If the crosslinking process associated with ethylene/propylene was predominant, an increase in the structural cohesion would be expected [65], which did not happen. On the other hand, if chain scission in PP was taking place at higher levels, reduced T_m would be expected, which did not happen. The aging effect on PPc and blends suggests complex interactions, since they are distinct components where specific interactions may take place. In the case of PPcr alone, practically, its thermal properties did not change, since it may contain additives that minimize sudden changes. However, when mixing virgin resin (PPc) with recycled (PPcr), complex interactions occurred, in a similar way as the appearance of white particles, as verified in SEM images. Table 2 shows that the crystallization temperature (T_c) of PPc, PPcr, and blends were close to 122.9 °C. Upon increasing the aging time, no significant change was verified. However, there was a reduction in the intensity and width of the crystallization peaks of PPc and blends, whereas PPcr did not change the crystallization profile.

According to Table 2, the degree of crystallinity (X_c) of unaged PPc was lower than PPcr, suggesting the lower molar mass of recycled material favored the macromolecular mobility and structural organization [63,66]. In PPc/PPcr, X_c was higher than PPc, suggesting PPcr directed to increased crystallinity. Reduced X_c was verified upon aging during 30 and 60 days for PPc and blends, which agrees with reduced energy for crystallizing, as

presented in the T_c peaks. In general, the thermo-oxidation aging trend to deteriorate the crystallinity, i.e., hampers the molecular ordering. An exception is valid for PP_{cr}, in which the thermal properties remained unchanged.

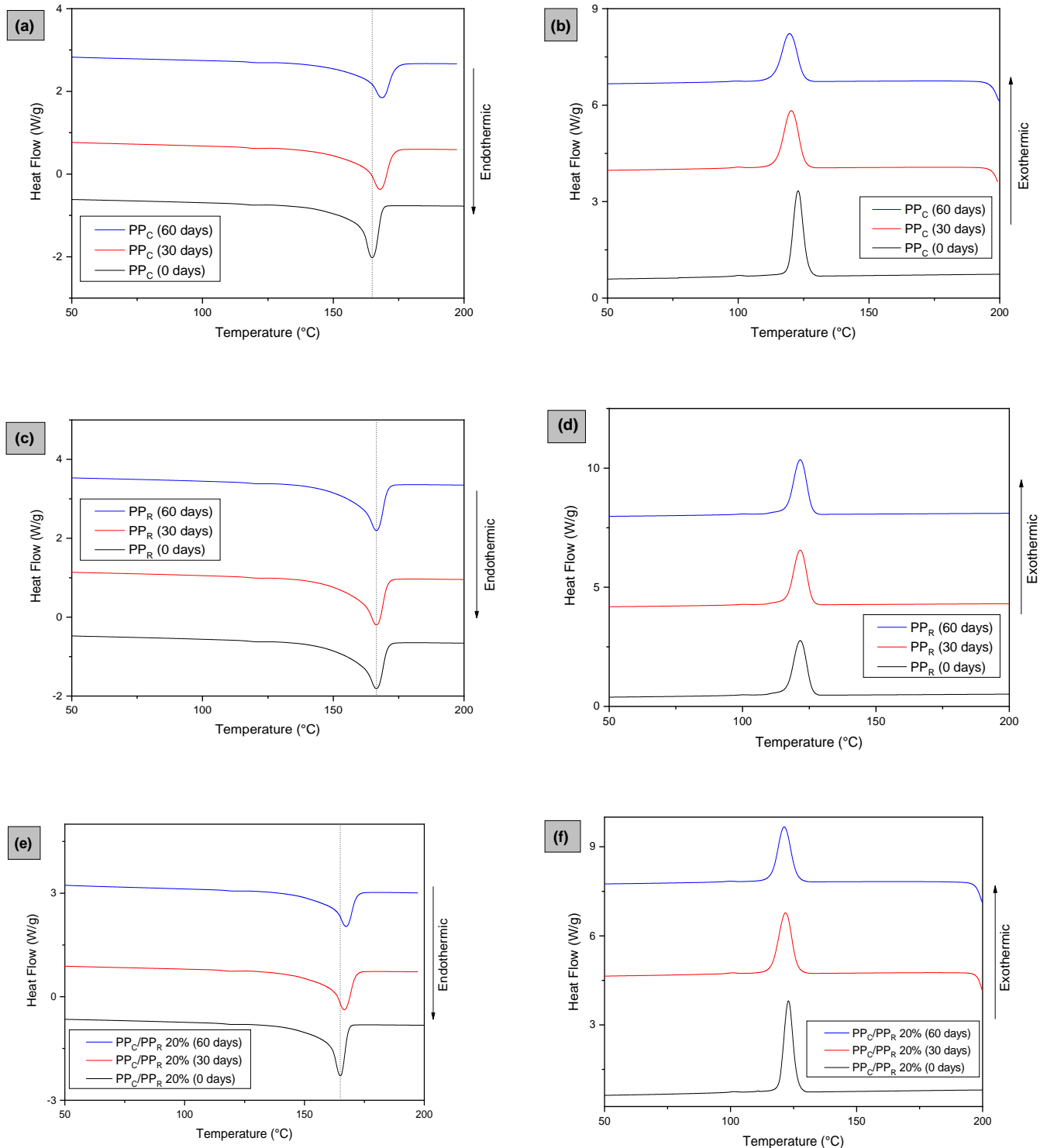


Figure 9. Cont.

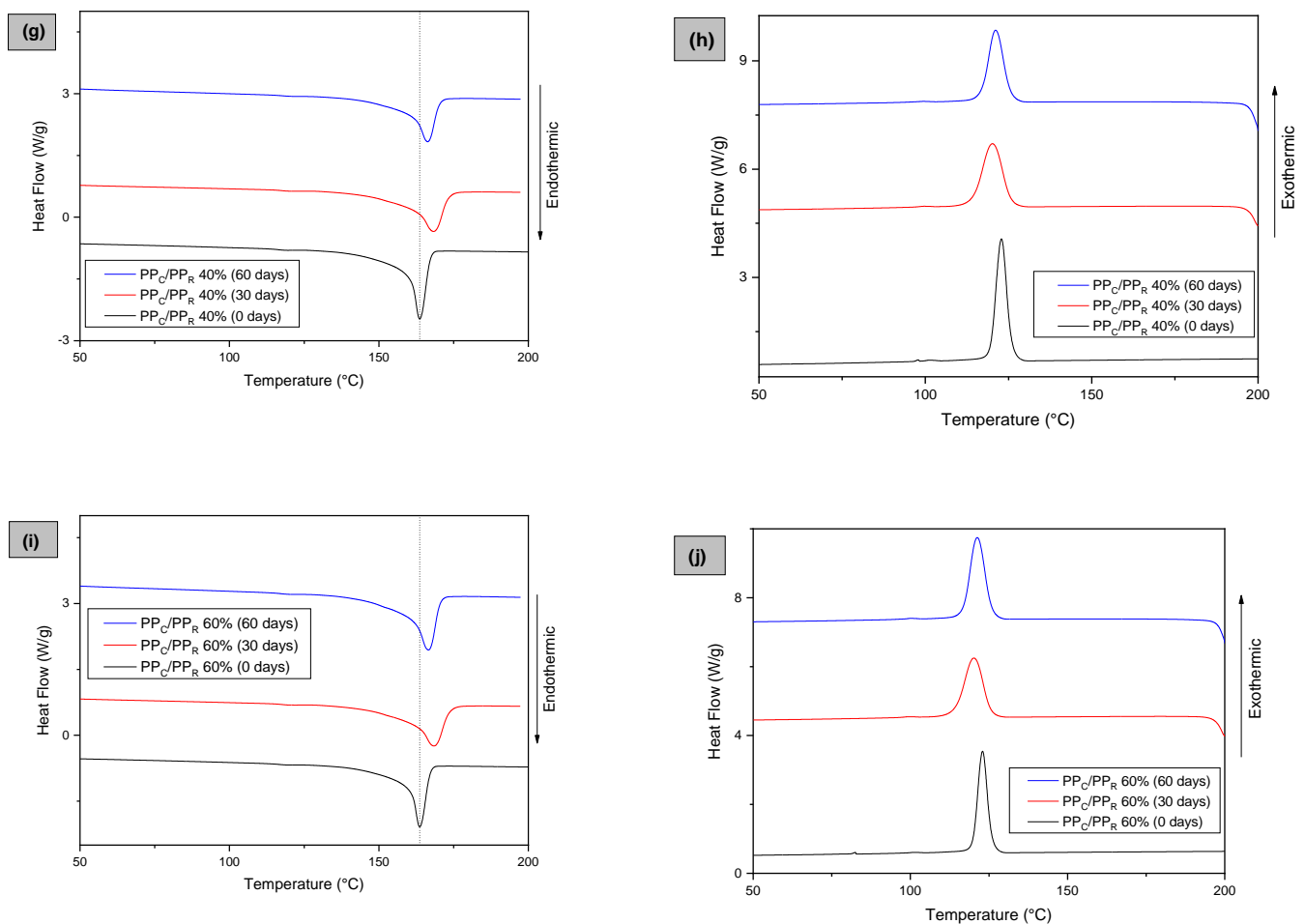


Figure 9. DSC scans for PPc, PPr, and PPc/PPr blends. (a,c,e,g,i) Melting endotherms. (b,d,f,h,j) Melt crystallization exotherms. Thermal aging indicated.

3.7. Impact Strength

Figure 10 shows impact strength as a function of thermo-oxidation aging for PPc, PPcr, and PPc/PPcr blends. Among non-aged samples, PPc presented the highest impact strength and PPcr presented the lowest one, while blends are between them. The lower impact strength of PPcr is mostly due to the reprocessing, which promotes chain scission and reduced molar weight [67], as shown in the MFI data (lower viscosity/higher MFI). A lower molar weight of PPcr decreases the molecular entanglements and, as a consequence, cracks quickly propagate. Nevertheless, upon the influence of thermo-oxidation aging, impact strength was lightly changed, which can be related to the chain scission mechanism, as well as the reduction in tangled macromolecular chains resulted from the lower molecular weight.

Figure 11 shows an impact strength ratio between t (30 and 60 days) (t_f) and time (0) (t_0), to better clarify changes in the impact of thermo-oxidation aging and compositions [68]. At 60 days of thermo-oxidation aging, the impact decreased, with PPc being the most damaged sample, whereas PPcr was the highest shielded against the harmful effects of thermo-oxidation degradation, reinforcing the hypothesis of possible protective additives (antioxidant). The effects of reprocessing and thermo-oxidative aging on post-consumption PP were investigated by Jansson et al. [69], and the different batches of recycled PP investigated differed substantially in mechanical properties, as well as in durability and potential recycling, which was attributed to the stabilizing additives typically used in PP, such as phenolic antioxidant and amines, in order to reduce the degradative effects. As already verified, blends presented impact data between those of PPc and PPcr, but also decreasing when the thermo-oxidation aging increased; in general, the addition of PPcr behaved as a

protector against the thermo-oxidation aging influence, mostly due to its stabilizer agents. Similarly, Fernandes et al. [70] observed this PP stabilizing action in PP/polystyrene (PS) blends exposed to ultraviolet (UV) radiation; as the reprocessed PP behaved in the same way, it was found that blends with PPcr showed better UV resistance.

Figure 11 reports that the addition of PPcr, up to 60%, to PPc did not damage the impact strength. At the same time, PPcr contributed to reduce the thermo-oxidation aging effects on the PPc matrix, suggesting that, despite being recycled material, it has proper properties. Reusing this post-consumption material is an important alternative for the development of sustainable and economical materials, since it contributes to the cost reduction of the final product [71].

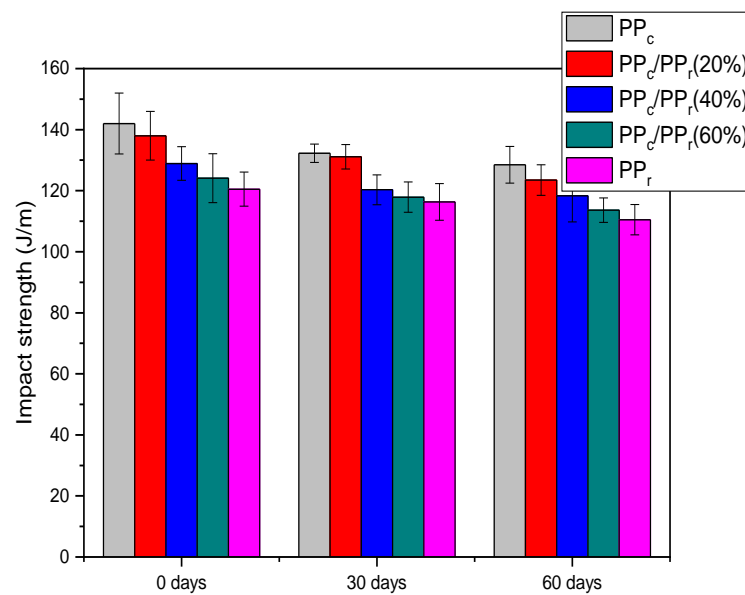


Figure 10. Impact strength of PPc, PPcr, and PPc/PPcr blends as a function of thermo-oxidation aging.

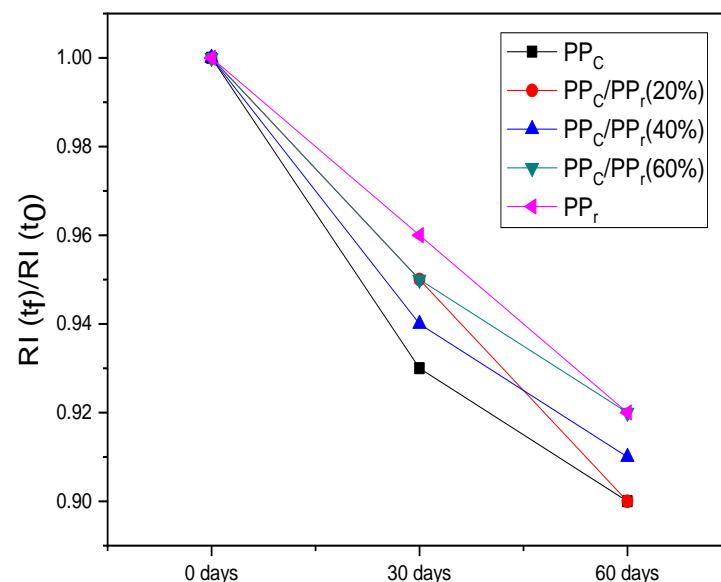


Figure 11. Impact strength ratio between time (30 and 60 days) (t_f) and time (0) (t_0), for PPc, PPcr, and PPc/PPcr blends.

3.8. Tensile Experiments

Figure 12 presents the elongation at break as a function of thermo-oxidation aging for PPc, PPcr, and PPc/PPcr blends. Non-aged specimens presented higher data, whereas PPc

had the highest value, possibly resulting from higher macromolecules, which provide able entanglements to lengthen during tensile [63,67]. PPcr presented poor elongation mechanisms, mostly due to a lower macro-molecular weight, which is unable to provide proper stretching. Following the trend already verified, PPc/PPcr blends presented elongation at break between neat polymers, decreasing upon PPcr increase; it is suggested, besides lower molecular weight, that there are fewer tie and tangled macromolecules in PPcr, thus reducing the capability to properly lengthen [72].

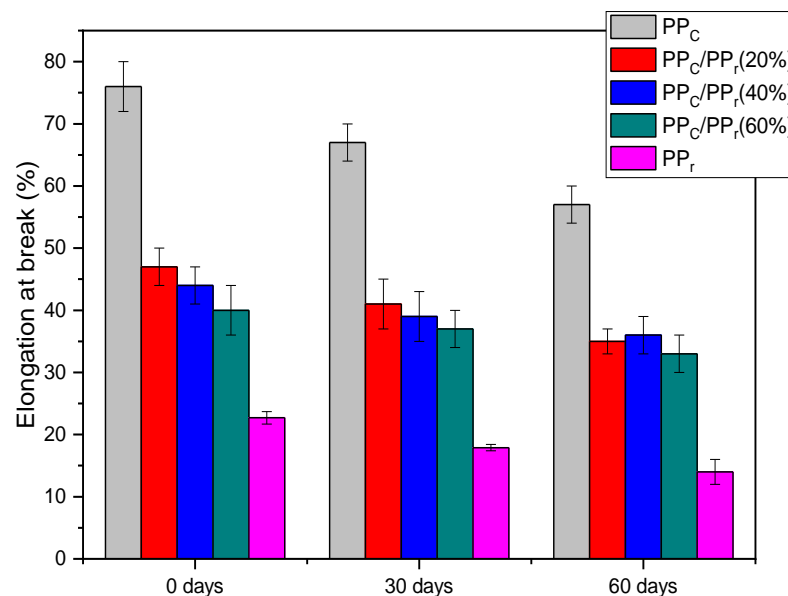


Figure 12. Elongation at break for PPc, PPcr, and blends as an aging function.

Regarding the effect of thermo-oxidation aging, PPc, PPcr, and PPc/PPcr presented lower performance in elongation at break, and upon thermo-oxidation degradation the progress samples underwent oxidative reactions, as verified in the FTIR, which resulted in chain scission, decreasing the elastic performance of tested specimens [70]. It is noteworthy to mention that most of the reactions occur in regions with higher oxygen availability, i.e., in the amorphous region [73]. The scission of tie molecules and reduction of tangles are the driving forces to reduce PP mechanical properties during aging. Generally, tie molecules' scission tends to decrease the elongation at break, since they would have to withstand an unbalanced mechanical stress [74].

In Figure 13, tensile strength data are shown, and the tested compounds presented subtle changes, regardless of the composition or thermo-oxidation aging influence. For non-aged specimens, PPcr displayed higher performance, which is believed to be related to two factors: (1) higher degree of crystallinity as seen in DSC; and (2) lower ethylene/propylene content (which is a flexible segment, thus greater content means greater deformation at lower stresses (reduces tensile strength); smaller content means higher stiffness, i.e., higher tensile tension to deform). Other non-aged blends presented data within the margin of experimental error. Having a look at PPc, for 30 days the tensile strength decreased, nevertheless, for 60 days it increased, which reinforces the hypothesis that chain scission and crosslinking reactions concomitantly occurred.

Elastic modulus, as a function of thermo-oxidation aging, is presented in Figure 14a, whereas the elastic modulus ratio measured at time t (30 and 60 days) (t_f) and time (0 days) (t_0) is in Figure 14b. In general, the elastic modulus was slightly changed, regardless of the composition or thermo-oxidation aging applied. Nevertheless, from a deeper view, in Figure 14b, it is clear PPcr presented a higher elastic modulus that increased with thermo-oxidation aging, mostly due to the higher degree of crystallinity and crosslinking reactions [60,70]. PPc and PPc/PPcr blends displayed a lower elastic modulus, which agrees with the impact and tensile strengths previously presented.

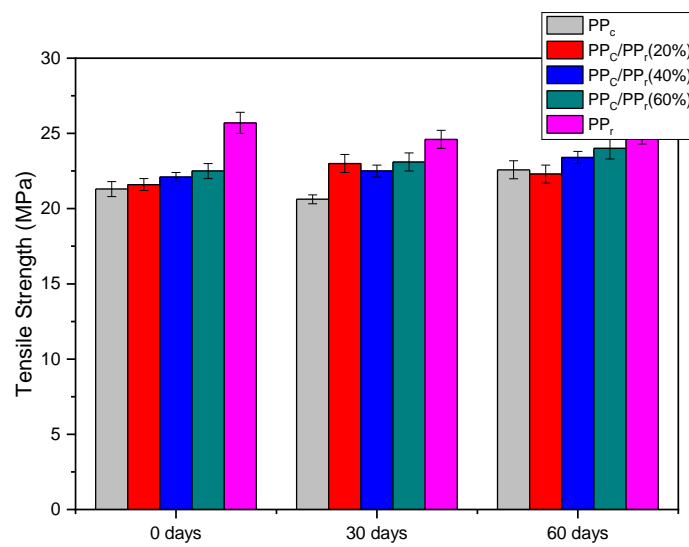


Figure 13. Tensile strength as a function of thermo-oxidation aging for PP_c, PP_cr, and PP_c/PP_cr blends.

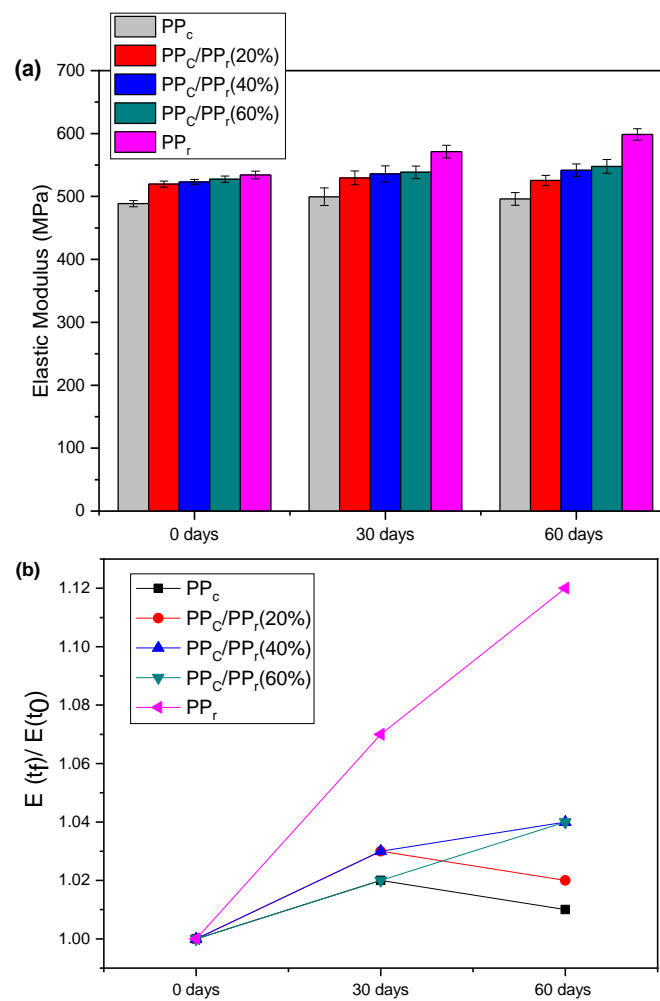


Figure 14. (a) Elastic modulus of PP_c, PP_cr, and PP_c/PP_cr blends, as a function of thermo-oxidation aging. (b) Ratio between elastic modulus at time (30 and 60 days) (t_f) and time (0 days) (t_0).

Figure 14b indicates that adding PP_cr to PP_c/PP_cr blends trended to minimize thermo-oxidation aging effects, providing greater stability in the elastic modulus. The performance

of PPc/PPcr blends upon aging is important, since the elastic modulus is one of the most important parameters of mechanical properties. Therefore, the improper disposal of PPcr, a raw material with technological potential for the recycling industry, may be viewed as throwing money away. In addition, PPcr contributes to the development of sustainable products with good properties, and it requires less energy and natural resources in its processing.

3.9. Stress versus Strain Analysis

Figure 15a–e shows the stress versus strain plots where ductile character, i.e., high deformation, is clearly verified for all experimented compounds. Analyzing PPc and PPcr plots, it is evident there are higher strains in the PPc ones; possibly, lower PPcr strains are linked to detrimental remnants from the previous processing, which decreased the molecular weight, impairing skillful deformation mechanisms. Blends' strains are compositionally dependent, decreasing upon PPcr content increase.

The area below the stress versus strain plot is defined as toughness, which is assumed as the material's ability to absorb energy until fracture; these areas were integrated and data are shown in Table 3. PPc presented the maximum area; among the tested compounds, it absorbs higher energy before fracturing, whereas PPcr, as the lowest area, has a feeble energy absorption mechanism, and toughness of PPc/PPcr blends depends on the PPc/PPcr ratio content, decreasing upon a PPcr content increase. Toughness data are in full agreement with impact strength (Figure 10), as already presented.

Table 3. Toughness of PPc, PPcr, and PPc/PPcr blends, measured from the stress versus strain area. Toughness was computed from the integrated area below the stress–strain plot, according to the equation, $T = \int_0^{\epsilon} \sigma d\epsilon$, where: ϵ and σ are strain and stress at fracture, respectively.

Compounds	Toughness (J)		
	0 Days	30 Days	60 Days
PP _C	1241.0	1061.2	941.3
PP _{CR}	343.1	284.3	235.4
PP _C /PP _{CR} (20%)	726.5	692.6	551.6
PP _C /PP _{CR} (40%)	712.6	699.2	607.5
PP _C /PP _{CR} (60%)	682.8	629.1	570.1

Related to the thermo-oxidation aging effect on the toughness of PPc, PPcr, and PPc/PPcr blends, reduction was observed, which increased with aging time. Thermo-oxidation degradation products are effective in damaging proper energy dissipation mechanisms, conducting a low toughness response.

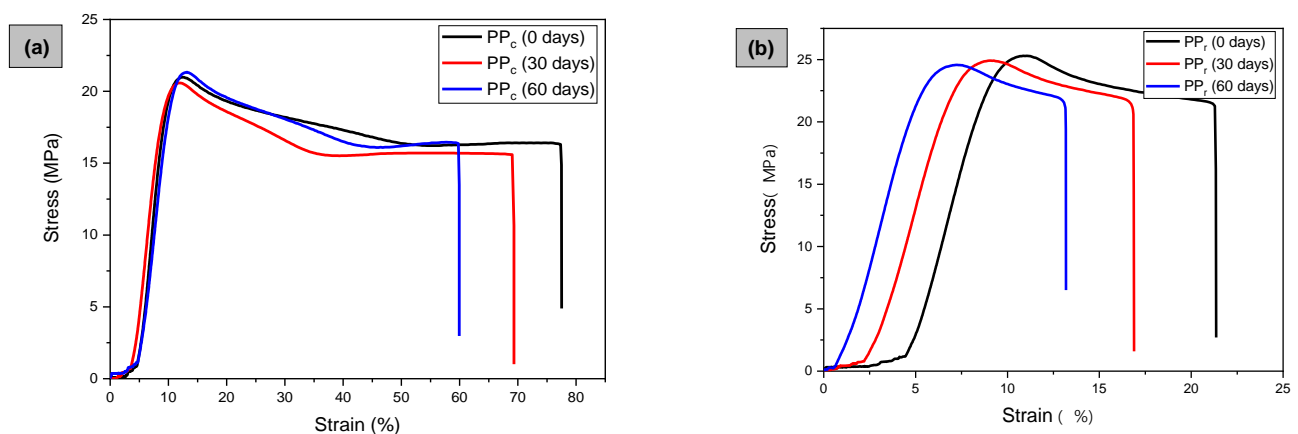


Figure 15. Cont.

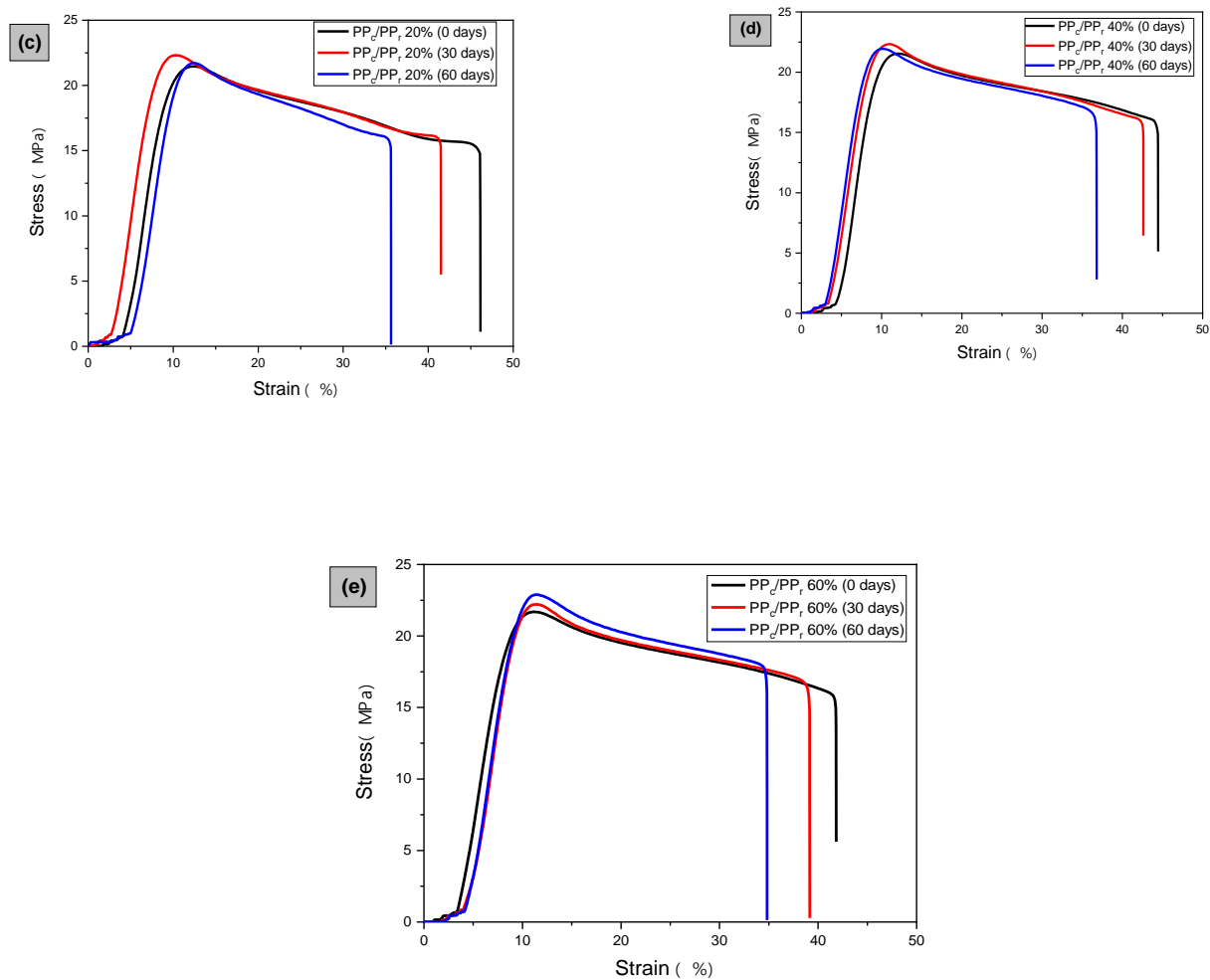


Figure 15. Stress versus strain plots of PPc, PPcr, and PPc/PPcr blends before and after aging.

3.10. Heat Deflection Temperature (HDT)

HDT is an important property for polymer technology, since it is used in quality control to measure dimensional stability [75,76]. Figure 16 shows HDT for PPc, PPcr, and PPc/PPcr blends, measured before and after thermo-oxidation aging. The HDT of PPcr increased due to a higher elastic modulus, as well as possible stabilizing agents. PPcr's HDT presented a higher parameter, mostly due to the possible added stabilizer agents and/or crosslinking reactions during reprocessing. HDT changes on aged and non-aged specimens are almost not noticeable, since the evaluated data are closely similar. Apparently, HDT was not affected by thermo-oxidation aging, which may be assumed as a very important result, i.e., the HDT of the blend was not affected by aging.

Adding high contents of PPcr did not compromise HDT, indicating an important technological contribution to PPc/PPcr blends. From the processing point of view, injection-molded PPc/PPcr blends can be removed from the mold at higher temperatures, as the structural deformation will be maintained at acceptable standards. Reusing PPcr has great potential for reintegration into the industrial production, which is interesting from both environmental and economic aspects.

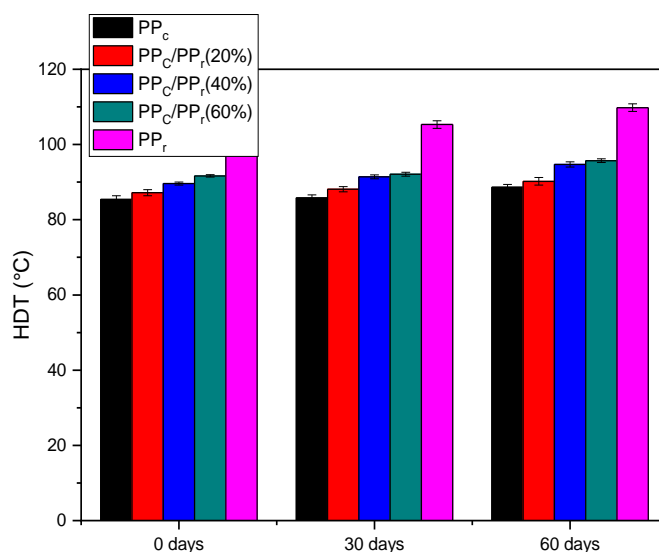


Figure 16. HDT of PP_c, PP_cr, and PP_c/PP_cr blends before and after thermo-oxidation aging.

4. Conclusions

The importance of PP_cr reusing is linked to sustainable development, which encompasses not only the environment, but also social and economic aspects. Using post-consumer PP_cr in the production cycle, value is added to the material, as well as reducing the costs of production and stimulating recycling growth. PP_c/PP_cr blends arose as a proper alternative for PP industrial applications, as the addition of PP_cr seemed to greatly minimize severe property losses, as verified through tensile strength and HDT. Despite decreasing blends' performance, thermo-oxidation aging was not expressively deleterious, and blends still settled with an adequate property balance after 60 days of aging. The acquired results of mechanical and thermomechanical properties are valuable for the recycling area, since the use of recycled PP can contribute to minimize the effects of thermo-oxidation aging in PP_c/PP_cr blends. In general, produced blends provide cost savings and, at the same time, favor a wide range of applications, such as toys, disposable pipettes, hair brushes, industrial containers, and products for general purposes.

Author Contributions: Conceptualization, C.B.B.L.; methodology, C.B.B.L., W.A.d.S. and L.J.M.D.d.S.; validation, C.B.B.L., E.M.A. and J.B.d.C.A.d.M.; formal analysis, C.B.B.L. and W.A.d.S.; investigation, C.B.B.L., W.A.d.S. and L.J.M.D.d.S.; resources, E.M.A. and J.B.d.C.A.d.M.; data curation, C.B.B.L., W.A.d.S. and R.M.R.W.; writing—original draft preparation, C.B.B.L. and R.M.R.W.; writing—review and editing, C.B.B.L. and R.M.R.W.; visualization, C.B.B.L., E.M.A. and J.B.d.C.A.d.M.; supervision, E.M.A. and J.B.d.C.A.d.M.; project administration, E.M.A.; funding acquisition, E.M.A. All authors have read and agreed to the published version of the manuscript.

Funding: This study was financed by the Coordenação de Aperfeiçoamento de Pessoal de Nível Superior—Brasil (CAPES)—Finance Code 001.

Institutional Review Board Statement: Not applicable.

Informed Consent Statement: Not applicable.

Data Availability Statement: Not applicable.

Acknowledgments: The authors would like to thank UFCG for the laboratory infrastructure, the National Council for Scientific and Technological Development-CNPq, Coordination for the Improvement of Higher Education Personnel (CAPES), for financial support, and the Northeastern Biomaterials Assessment and Development Laboratory (CERTBIO) for the FTIR and MFI analyses.

Conflicts of Interest: The authors declare no potential conflict of interest with respect to the research, authorship, and/or publication of this article.

References

1. Mbarek, S.; Baccouch, Z.; Eterradossi, O.; Perrin, D.; Monasse, B.; Garay, H.; Quantin, J.C. Effect of recycling and injection parameters on gloss properties of smooth colored polypropylene parts: Contribution of surface and skin layer. *Polym. Eng. Sci.* **2019**, *59*, 1288–1299. [[CrossRef](#)]
2. Alves, A.M.; Cavalcanti, S.N.; Arimatéia, R.R.; Agrawal, P.; Freitas, N.L.; Mélo, T.J.A. Influência do processamento e da alumina sintetizada em laboratório nas propriedades do polipropileno. *Rev. Eletrônica Mater. Processos* **2016**, *11*, 155–163.
3. Luna, C.B.B.; Siqueira, D.D.; Araújo, E.M.; Wellen, R.M.R. Tailoring PS/PPrecycled blends compatibilized with SEBS. Evaluation of rheological, mechanical, thermomechanical and morphological character. *Mater. Res. Express* **2019**, *6*, 075316. [[CrossRef](#)]
4. Grigorescu, R.M.; Ghioca, P.; Lancu, L.; David, M.E.; Andrei, E.R.; Filipescu, M.L.; Lon, R.M.; Vuluga, Z.; Anghel, L.; Sofran, L.E.; et al. Development of thermoplastic composites based on recycled polypropylene and waste printed circuit boards. *Waste Manag.* **2020**, *118*, 391–401. [[CrossRef](#)]
5. Aumnate, C.; Rudolph, N.; Sarmadi, M. Recycling of polypropylene/polyethylene blends: Effect of chain structure on the crystallization behaviors. *Polymers* **2019**, *11*, 1456. [[CrossRef](#)]
6. Galve, J.E.; Elduque, D.; Pina, C.; Clavería, I.; Acero, R.; Fernández, A.; Javierre, C. Dimensional Stability and Process Capability of an Industrial Component Injected with Recycled Polypropylene. *Polymers* **2019**, *11*, 1063. [[CrossRef](#)]
7. Matias, A.A.; Lima, M.S.; Pereira, J.; Pereira, P.; Barros, R.; Coelho, J.F.J.; Serra, A.C. Use of recycled polypropylene/poly(ethylene terephthalate) blends to manufacture water pipes: An industrial scale study. *Waste Manag.* **2020**, *101*, 250–258. [[CrossRef](#)]
8. Camargo, R.V.; Saron, C. Mechanical–chemical recycling of low-density polyethylene waste with polypropylene. *J. Polym. Environ.* **2019**, *28*, 794–802. [[CrossRef](#)]
9. Beltrán, F.R.; Barrio, L.; Lorenzo, V.; Río, D.; Urreaga, J.M.; Orden, M.U. Valorization of poly(lactic acid) wastes via mechanical recycling: Improvement of the properties of the recycled polymer. *Waste Manag. Res.* **2018**, *37*, 135–141. [[CrossRef](#)]
10. Luna, C.B.B.; Siqueira, D.D.; Ferreira, E.S.B.; Silva, W.A.; Nogueira, J.A.S.; Araújo, E.M. From Disposal to Technological Potential: Reuse of Polypropylene Waste from Industrial Containers as a Polystyrene Impact Modifier. *Sustainability* **2020**, *12*, 5272. [[CrossRef](#)]
11. Taghavi, S.K.; Shahrajabian, H.; Hosseini, H.M. Detailed comparison of compatibilizers MAPE and SEBS-g-MA on the mechanical/thermal properties, and morphology in ternary blend of recycled PET/HDPE/MAPE and recycled PET/HDPE/SEBS-g-MA. *J. Elastomers Plast.* **2017**, *50*, 13–35. [[CrossRef](#)]
12. Rajasekaran, D.; Maji, P.K. Recycling of Quaternary Household Plastic Wastes by Utilizing Poly(Ethylene-co-Methacrylic acid) Copolymer Sodium Ion: Compatibility and Re-processability Assessments. *J. Polym. Environ.* **2019**, *28*, 471–482. [[CrossRef](#)]
13. Overcash, M.R.; Ewell, J.H.; Griffing, E.M. Life cycle energy comparison of different polymer recycling processes. *J. Adv. Manuf. Process.* **2020**, *2*, e10034. [[CrossRef](#)]
14. Kaiser, K.; Schmid, M.; Schlummer, M. Recycling of Polymer-Based Multilayer Packaging: A Review. *Recycling* **2018**, *3*, 1. [[CrossRef](#)]
15. Araújo, L.M.G.; Morales, A.R. Compatibilization of recycled polypropylene and recycled poly (ethylene terephthalate) blends with SEBS-g-MA. *Polímeros Ciência Tecnol.* **2018**, *28*, 84–91. [[CrossRef](#)]
16. Luna, C.B.B.; Silva, D.F.; Araújo, E.M. Estudo do comportamento de blendas de polimiada 6/resíduos de borracha da indústria de calçados. *Rev. Univap* **2014**, *20*, 98–110. [[CrossRef](#)]
17. Adam, A.P.; Gonçalves, J.V.R.V.; Robinson, L.C.; Da Rosa, L.C.; Schneider, E.L. Recycling and Mechanical Characterization of Polymer Blends Present in Printers. *Mater. Res.* **2017**, *20*, 202–208. [[CrossRef](#)]
18. Hanna, E.G. Recycling of waste mixed plastics blends (PE/PP). *J. Eng. Sci. Technol. Rev.* **2019**, *12*, 87–92. [[CrossRef](#)]
19. Santos, L.S.; Silva, A.H.M.F.T.; Pacheco, E.B.A.V.; Silva, A.L.N. Study of the effect of recycled PP on the mechanical and flow properties of PP/EPDM blends. *Polímeros Ciência Tecnol.* **2013**, *23*, 389–394. [[CrossRef](#)]
20. Ferreira, E.S.B.; Pereira, C.H.O.; Araújo, E.M.; Bezerra, E.B.; Siqueira, D.D.; Wellen, R.M.R. Properties and morphology of polypropylene/big bags compounds. *Mater. Res.* **2019**, *22*, 1–8. [[CrossRef](#)]
21. Fernandes, B.L.; Domingues, A.J. Mechanical characterization of recycled polypropylene for automotive industry. *Polímeros Ciência Tecnol.* **2007**, *17*, 85–87. [[CrossRef](#)]
22. Barbosa, L.G.; Piaia, M.; Ceni, G.H. Analysis of impact and tensile properties of recycled polypropylene. *Int. J. Mater. Eng.* **2017**, *7*, 117–120. [[CrossRef](#)]
23. Alcântara, R.L.; Carvalho, L.H.; Ramos, S.M.L.S. Propriedades mecânicas de resíduos plásticos urbanos da região nordeste. 1- Influência das condições de processamento. *Polímeros* **1995**, *5*, 42–47.
24. Solis, M.; Silveira, S. Technologies for chemical recycling of household plastics—A technical review and TRL assessment. *Waste Manag.* **2020**, *105*, 128–138. [[CrossRef](#)]
25. Callister, W.D. *Ciência e Engenharia de Materiais: Uma Introdução*; LTC: Rio de Janeiro, Brazil, 2011; Volume 7, p. 572.
26. Gijssman, P.; Kroon, M.; Oorschot, M. The role of peroxides in the thermooxidative degradation of polypropylene. *Polym. Degrad. Stab.* **1996**, *51*, 3–13. [[CrossRef](#)]
27. Hamida, H.M.A. Effect of electron beam irradiation on polypropylene films—Dielectric and FT-IR studies. *Solid State Electron.* **2005**, *49*, 1163–1167. [[CrossRef](#)]

28. Nogueira, L.M.; Dutra, R.C.L.; Diniz, M.F.; Pires, M.; Evangelista, M.; Santana, F.A.; Tomasi, L.; Santos, P.; Nonemacher, R. Evaluation of MIC/FT-IR/DSC techniques for multilayer films characterization. *Polímeros Ciência E Tecnol.* **2007**, *17*, 158–165. [[CrossRef](#)]
29. Shen, Y.; Wu, P. Two-dimensional ATR–FTIR spectroscopic investigation on water diffusion in polypropylene film: Water bending vibration. *J. Phys. Chem. B* **2003**, *107*, 4224–4226. [[CrossRef](#)]
30. Paoli, M.A. *Degradation and Stabilization of Polymers*; Artliber Editora: São Paulo, Brazil, 2008.
31. Xiang, Q.; Xanthos, M.; Patel, S.H.; Mitra, S. Comparison of volatile emissions and structural changes of melt reprocessed polypropylene resins. *Adv. Polym. Technol.* **2002**, *21*, 235–242. [[CrossRef](#)]
32. Brito, R.S.F.; Silva, S.M.L.; Rabello, M.S. Controle da fotodegradação de PP pigmentado pelo uso de fotoestabilizantes. *Rev. Eletrônica Mater. Processos* **2016**, *11*, 73–80.
33. Xiang, Q.; Xanthos, M.; Mitra, S.; Patel, S.H.; Guo, J. Effects of melt reprocessing on volatile emissions and structural/rheological changes of unstabilized polypropylene. *Polym. Degrad. Stab.* **2002**, *77*, 93–102. [[CrossRef](#)]
34. Rabello, M.S. *Polymers Additives*; Artliber Editora: São Paulo, Brazil, 2000.
35. Gugumus, F. Thermooxidative degradation of polyolefins in the solid state—Kinetics of thermal oxidation of polypropylene. *Polym. Degrad. Stab.* **1998**, *62*, 235–243. [[CrossRef](#)]
36. Cavalcanti, R.S.F.B.; Rabello, M.S. The effect of red pigment and photo stabilizers on the photo degradation of polypropylene films. *Mater. Res.* **2019**, *22*, 1–8. [[CrossRef](#)]
37. Khabbaz, F.; Albertsson, A.C. Rapid test methods for analyzing degradable polyolefins with a pro-oxidant system. *J. Appl. Polym. Sci.* **2001**, *79*, 2309–2316. [[CrossRef](#)]
38. Hjertberg, T.; Palmlof, M.; Sultan, B.A. Chemical reactions in crosslinking of copolymers of ethylene and vinyltrimethoxy silane. *J. Appl. Polym. Sci.* **1991**, *42*, 1185–1192. [[CrossRef](#)]
39. Sen, A.K.; Mukherjee, B.; Bhattacharyya, A.S.; De, P.P.; Bhowmick, A.K. Kinetics of silane grafting and moisture crosslinking of polyethylene and ethylene propylene rubber. *J. Appl. Polym. Sci.* **1992**, *44*, 1153–1164. [[CrossRef](#)]
40. Fechine, G.J.M.; Santos, J.A.B.; Rabello, M.S. The evaluation of polyolefin photodegradation with natural and artificial exposure. *Química Nova* **2006**, *29*, 674–680. [[CrossRef](#)]
41. Ol'khov, A.A.; Shibryaeva, L.S.; Tertyshnaya, Y.V.; Kovaleva, A.N.; Kucherenko, E.L.; Zhul'kina, A.L.; Iordanskii, A.L. Resistance to thermal oxidation of ethylene-propylene rubber and polyhydroxybutyrate blends. *Int. Polym. Sci. Technol.* **2017**, *44*, 11–14. [[CrossRef](#)]
42. Tochacek, J.; Jancar, J.; Kalfus, J.; Zborilova, P.; Burán, Z. Degradation of polypropylene impact-copolymer during processing. *Polym. Degrad. Stab.* **2008**, *93*, 770–775. [[CrossRef](#)]
43. Severini, F. Environmental Degradation of Polypropylene. *Polym. Degrad. Stab.* **1988**, *22*, 185–194. [[CrossRef](#)]
44. Pandey, J.K.; Ahamda, A.; Singh, R.P. Ecofriendly behavior of host matrix in composites prepared from agro-waste and polypropylene. *J. Appl. Polym. Sci.* **2003**, *90*, 1009–1017. [[CrossRef](#)]
45. Waldman, W.R.; Paoli, M.A. Photodegradation of polypropylene/polystyrene blends: Styrene–butadiene–styrene compatibilisation effect. *Polym. Degrad. Stab.* **2008**, *93*, 273–280. [[CrossRef](#)]
46. Nasir, A.; Yasin, T.; Islam, A. Thermo-oxidative degradation behavior of recycled polypropylene. *J. Appl. Polym. Sci.* **2011**, *119*, 3315–3320. [[CrossRef](#)]
47. Hebbbar, R.S.; Isloor, A.M.; Ismail, A.F. Contact angle measurements. *Membr. Charact.* **2017**, *1*, 219–255.
48. Luna, C.B.B.; Siqueira, D.D.; Ferreira, E.S.B.; Araújo, E.M.; Wellen, R.M.R. Reactive compatibilization as a proper tool to improve PA6 toughness. *Mater. Res. Express* **2019**, *6*, 125367. [[CrossRef](#)]
49. Matsunaga, M.; Whitney, P.J. Surface changes brought about by corona discharge treatment of polyethylene film and the effect on subsequent microbial colonization. *Polym. Degrad. Stab.* **2000**, *70*, 325–332. [[CrossRef](#)]
50. Gensler, R.; Plummer, C.J.G.; Kausch, H.H.; Kramer, E.; Pauquet, J.R.; Zweifel, H. Thermo-oxidative degradation of isotactic polypropylene at high temperatures: Phenolic antioxidants versus HAS. *Polym. Degrad. Stab.* **2000**, *67*, 195–2081. [[CrossRef](#)]
51. Ribeiro, V.F.; Júnior, N.S.D.; Riegel, I.C. Recovering properties of recycled HIPS through incorporation of SBS triblock copolymer. *Polímeros Ciência Tecnol.* **2012**, *22*, 186–192. [[CrossRef](#)]
52. Lotti, C.; Correa, C.A.; Canevarolo, S.V. Mechanical and morphological characterization of polypropylene toughened with olefinic elastomer. *Mater. Res.* **2000**, *3*, 37–44. [[CrossRef](#)]
53. Martuscelli, E. Structure and properties of polypropylene elastomer blends. In *Polypropylene Structure, Blends and Composites*; Karger-Kocsis, J., Ed.; Springer: Dordrecht, The Netherlands, 1995; pp. 95–140.
54. Bedia, E.L.; Astrini, N.; Sudarisman, A.; Sumera, F.; Kashiro, Y. Characterization of polypropylene and ethylene–propylene copolymer blends for industrial applications. *J. Appl. Polym. Sci.* **2000**, *78*, 1200–1208. [[CrossRef](#)]
55. Cáceres, C.A.; Canevarolo, S.V. Polypropylene degradation during extrusion and the formation of volatile organic compounds. *Polímeros Ciência Tecnol.* **2009**, *19*, 79–84. [[CrossRef](#)]
56. González, V.A.G.; Velázquez, G.N.; Sánchez, J.L.A. Polypropylene chain scissions and molecular weight changes in multiple extrusion. *Polym. Degrad. Stab.* **1998**, *60*, 33–42. [[CrossRef](#)]
57. Fechine, G.J.M.; Demarquette, N.R. Cracking formation on the surface of extruded photodegraded polypropylene plates. *Polym. Eng. Sci.* **2008**, *48*, 365–372. [[CrossRef](#)]

58. Rabello, M.S.; White, J.R. The role of physical structure and morphology in the photodegradation behavior of polypropylene. *Polym. Degrad. Stab.* **1997**, *56*, 55–73. [[CrossRef](#)]
59. Makhlis, F.A. *Radiation Physics and Chemistry of Polymers*; John Wiley & Sons: Jerusalem, Israel, 1975.
60. Geuskens, G. New aspects of the photo-oxidation and photo-stalization os polymers. *Macromol. Symp.* **1989**, *27*, 85–96. [[CrossRef](#)]
61. Men, R.; Lei, Z.; Song, J.; Li, Y.; Lin, L.; Tian, M. Effect of thermal ageing on space charge in ethylene propylene rubber at DC voltage. *IEEE Trans. Dielectr. Electr. Insul.* **2019**, *26*, 792–800. [[CrossRef](#)]
62. Luna, C.B.B.; Ferreira, E.S.B.; Siqueira, D.D.; Silva, W.A.; Araújo, E.M.; Wellen, R.M.R. Tailoring performance of PP/HIPS/SEBS through blending design. *Mater. Res. Express* **2019**, *6*, 115321. [[CrossRef](#)]
63. Aurrekoetxea, J.; Sarrionandia, M.A.; Urrutibeascoa, I.; MasPOCH, M.L. Effects of recycling on the microstructure and the mechanical properties of isotactic polypropylene. *J. Mater. Sci.* **2001**, *36*, 2607–2613. [[CrossRef](#)]
64. Belkoucem, K.; Benarab, A.; Krache, R.; Benavente, R.; Pérez, E.; Cerrada, M.L. Effect of thermal treatment on the mechanical and viscoelastic response of polypropylenes incorporating a β nucleating agent. *J. Elastomers Plast.* **2018**, *51*, 562–579. [[CrossRef](#)]
65. Billmeyer, F.W. *Textbook of Polymer Science*; John Wiley & Sons: New York, NY, USA, 1984.
66. Martins, M.H.; Paoli, M.A. Polypropylene compounding with post-consumer material: II. Reprocessing. *Polym. Degrad. Stab.* **2002**, *78*, 491–495. [[CrossRef](#)]
67. Martins, M.H.; De Paoli, M.A. Polypropylene compounding with recycled material I. Statistical response surface analysis. *Polym. Degrad. Stab.* **2001**, *71*, 293–298. [[CrossRef](#)]
68. Saron, C.; Sanchez, E.M.S.; Isabel Felisberti, M. Thermal and photochemical degradation of PPO/HIPS blends. *J. Appl. Polym. Sci.* **2007**, *104*, 3269–3276. [[CrossRef](#)]
69. Jansson, A.; Moller, K.; Gevert, T. Degradation of post-consumer polypropylene materials exposed to simulated recycling—Mechanical properties. *Polym. Degrad. Stab.* **2003**, *82*, 37–46. [[CrossRef](#)]
70. Fernandes, L.L.; Freitas, C.A.; Demarquette, N.R.; Fachine, G.J.M. Photodegradation of thermodegraded polypropylene/high-impact polystyrene blends: Mechanical properties. *J. Appl. Polym. Sci.* **2011**, *120*, 770–779. [[CrossRef](#)]
71. Pacheco, E.B.; Hemais, C.A. Market for PET/HDPE/Ionomer recycled products. *Polímeros* **1999**, *9*, 59–64. [[CrossRef](#)]
72. Bahlouli, N.; Pessey, D.; Raveyre, C.; Guillet, J.; Ahzi, S.; Dahoun, A.; Hiver, J.M. Recycling effects on the rheological and thermomechanical properties of polypropylene-based composites. *Mater. Des.* **2012**, *33*, 451–458. [[CrossRef](#)]
73. Fernandes, L.L.; Freitas, C.A.; Demarquette, N.R.; Fachine, G.J.M. Estudo do efeito do tipo de polipropileno na fotodegradação da blenda polipropileno/poliestireno de alto impacto. *Polímeros* **2012**, *22*, 61–68. [[CrossRef](#)]
74. Rabello, M.S.; White, J.R. Fotodegradação do polipropileno. Um Processo essencialmente heterogêneo. *Polímeros* **1997**, *7*, 47–57. [[CrossRef](#)]
75. Takemori, M.T. Towards an understanding of the heat distortion temperature of thermoplastics. *Polym. Eng. Sci.* **1979**, *19*, 1104–1109. [[CrossRef](#)]
76. Luna, C.B.B.; Silva, D.F.; Araújo, E.M. Efeito dos agentes de compatibilização SBS e SEBS-MA no desempenho de misturas de poliestireno/resíduo de borracha de SBR. *Matéria* **2016**, *21*, 632–646. [[CrossRef](#)]